International Journal of Coal Geology 280 (2023) 104400

Contents lists available at ScienceDirect

International Journal of Coal Geology

journal homepage: www.elsevier.com/locate/coal

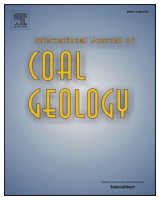

CFD modelling of longwall goaf atmosphere under vertical boreholes gas drainage

Yuehan Wang [a], Guangyao Si [a,*], Joung Oh [a], Bharath Belle [a,b,c,d]

[a] School of Minerals and Energy Resources Engineering, University of New South Wales, Sydney, NSW 2052, Australia
[b] School of Mechanical & Mining Engineering, University of Queensland, Brisbane QLD4072, Australia
[c] University of Pretoria, South Africa
[d] Anglo American Steelmaking Coal, Brisbane, QLD 4001, Australia

ARTICLE INFO

Keywords:
CFD modelling
Goaf gas drainage
Vertical boreholes
Longwall goaf atmosphere
Natural goaf characteristics

ABSTRACT

To effectively control and utilise large amounts of gas emissions from underground coal mining, Australia and many other countries rely heavily on a series of vertical boreholes to capture the gas during mining. This gas capture not only reduces the greenhouse gas impact but also recovers a significant amount of energy. Vacuum pumps are connected to surface boreholes to drive gas flow from the goaf and overlying fractured strata. However, applying high suction pressure to the boreholes may cause more oxygen to enter the goaf from the longwall working face. This influx of oxygen can potentially react with residual coal in the goaf, accelerating coal self-heating and possibly resulting in endogenous fires. By analysing extensive goaf gas drainage data collected from Australian longwalls, researchers have established the normal trend of goaf gas concentration and flow rate as a result of intensive goaf gas drainage. This paper further developed goaf gas flow CFD models with the operating vertical boreholes, which were then calibrated using field borehole production data under certain operating conditions. The CFD model simulated the distribution of O_2 and CH_4 as well as the gas flow pathways in the goaf, considering the complication of goaf gas drainage. This study found that the O_2 concentration is higher on the goaf tailgate side under the influence of tailgate side boreholes compared to the maingate side. Furthermore, for the well-compacted goaf, a significant proportion of the ventilation air travels through 'high permeability flow channels' provided by the goaf edge on tailgate side, and then circulates back into the goaf boreholes. These CFD modelling results not only enable ventilation engineers to visualize the goaf gas flow patterns under the impact of multiple operating boreholes, but also to understand the impact on goaf atmosphere through sensitivity analysis of natural goaf characteristics, such as goaf permeability distributions and gas emission rates.

1. Introduction

Longwall mining is a highly productive method of underground coal mining that involves extracting coal in long panels or faces. In this method, a longwall working face is formed using a shearer that moves back and forth along the face. As the shearer moves, it cuts the coal and loads it onto a conveyor for transportation. The longwall face is supported by hydraulic-powered roof supports as it advances, allowing the overlying strata to collapse behind it. This process is repeated until the longwall face reaches the end of a planned longwall panel (Karacan et al., 2007a; Szurgacz and Brodny, 2020; Tutak et al., 2020). This method is used in many countries around the world due to its efficiency, but it also poses several challenges related to safety, environmental impacts, and economic viability.

One of the significant safety and environmental concerns associated with longwall mining is the release of methane gas from the coal seam and the goaf (the mined area behind the longwall face where the coal has been extracted) (Si et al., 2015a; Si et al., 2015b; Tutak and Brodny, 2017; Brodny and Tutak, 2021). Longwall gas emissions are constantly increasing due to high retreat rates, high gas content in coal seams, and increased width and length of longwall panels (Balusu et al., 2005; Tanguturi et al., 2012). Since methane is a potent greenhouse gas that can also be explosive, its removal is necessary for both safety and environmental reasons. Various techniques have been developed to

* Corresponding author.
E-mail address: g.si@unsw.edu.au (G. Si).

https://doi.org/10.1016/j.coal.2023.104400
Received 9 September 2023; Received in revised form 30 October 2023; Accepted 18 November 2023
Available online 22 November 2023
0166-5162/© 2023 The Authors. Published by Elsevier B.V. This is an open access article under the CC BY license (http://creativecommons.org/licenses/by/4.0/).

mitigate methane emissions from longwall mining, including horizontal boreholes, vertical boreholes, and cross-measure boreholes (Karacan et al., 2011; Karacan, 2009b). In Australian underground coal mines, goaf gas drainage from vertical boreholes is widely used to address this issue when the overlying strata collapse into the goaf. This method involves drilling a series of vertical boreholes from the surface to a certain depth (usually 10 m to 20 m above the mining level) to extract gas emissions from the goaf and overlying fractured strata. Furthermore, this method reduces the amount of goaf gas released into the atmosphere and keeps methane concentrations in underground mining workplaces under the required statutory limits. Goaf gas drainage from vertical boreholes not only recovers high-purity gas from multiple coal seams as a source of energy but also reduces longwall production delays caused by gas exceedance at the tailgate. Consequently, goaf gas drainage has become an essential part of controlling longwall gas emissions in Australia. As mining operations go deeper and generate higher gas emissions, coal mines in Australia are adopting more aggressive goaf drainage designs. These designs involve narrower spacing between boreholes and the application of stronger suction pressure on the surface. As a result, these boreholes can draw more ventilation air back into the goaf during longwall mining. It can also cause leaked air to react with the residual coal in the goaf and gradually accumulate heat due to the low airflow rate, which may increase the risk of spontaneous combustion and gas explosion (Liu et al., 2011; Yang et al., 2014). To optimize goaf gas drainage efficiency and ensure underground goaf safety, it is necessary to understand the mechanisms of ventilation air/gas migration in the longwall goaf and the influence of various parameters on the goaf atmosphere.

The longwall goaf atmosphere and gas flow patterns are impacted by various natural characteristics, including goaf permeability and porosity distribution, gas emissions, and longwall ventilation systems. Guo et al. (2012) identified three primary factors that can influence goaf gas drainage performance: the distribution of permeability in the goaf, the degree of stress relief, and the goaf gas flow pattern. The permeability distribution, which is critical in controlling gas release and migration, is largely determined by the compaction degree in the goaf caved and fractured zones after longwall coal extraction (Brodny et al., 2018; Liu et al., 2021). To estimate the goaf permeability distribution, researchers (Esterhuizen and Karacan, 2005, 2007; Karacan et al., 2007a; Karacan et al., 2012) developed geomechanical models to simulate progressive coal extraction and goaf compaction, with the output stress information used to calculate goaf permeability. The permeability data are then used in gas reservoir flow models to evaluate goaf gas drainage performance (Karacan et al., 2007a; Karacan, 2009). Wachel (2012) conducted goaf compaction studies using FLAC3D model to establish longwall goaf porosity for western U.S. coal mines. The modelling results showed that the goaf compaction was non-uniform, and the porosity of the goaf varied by depths and locations. Besides, the detailed permeability and stress distributions were then investigated by Guo et al. (2012) using numerical modelling, specifically through COSFLOW modelling. Their findings indicated that permeability increased at the stress-relief zone, and an “annular” zone with high vertical and horizontal permeability was created in the goaf area. Moreover, Wang et al. (2022a, 2022b) proposed a theoretical goaf resistance model using a large amount of field data to estimate the goaf permeability. The research shows that the permeability decreases firstly along the face-to-hole distance and tends to be stable after the goaf is completely compacted. Additionally, some Chinese researchers (Gao and Wang, 2010; Gao et al., 2013) also reported that the distribution of permeability can have an impact on the airflow pathways and gas distribution within the longwall goaf.

With the advancement of computer calculation efficiency, numerical models have been widely used to comprehend gas emissions and evaluate the performance of goaf gas drainage in longwall mining. Tomita et al. (2003) established a finite element model to predict the amount of methane released by the surrounding coal seams and strata based on stress distribution and permeability changes. This model allowed for the prediction of gas emissions in different mining scenarios and provide a better understanding of the mechanisms of gas migration in the goaf. Besides, geomechanical and reservoir models were developed by Karacan et al. (2007b) to study the influence of the width of the longwall panel on methane emissions and assess the most effective borehole design that can maximise methane capture, while preventing gas from entering the underground workings. Karacan et al., 2006, 2007a, 2007b; Karacan, 2009c) also proposed a reservoir simulation model to study the influence of borehole design and operating conditions on the performance of goaf gas drainage. These studies mostly aim to improve drainage efficiency by analysing the gas emission reservoir conditions and optimising the goaf gas drainage designs. However, the distribution of the borehole captured gas in the goaf and how it evolves during the borehole operation period has not been well understood.

Computational Fluid Dynamics (CFD) modelling has been used to understand gas mixture behaviours and the complex gas flow patterns in the longwall goaf by many researchers in recent decades. Balusu et al. (2002, 2004, 2005) conducted industry supported CFD studies of goaf gas flow to develop gas and spontaneous combustion control strategies for a highly gassy mine. As Fig. 1 shows, the O_2 has a higher concentration and travels farther away from the face into the goaf at the maingate side, compared with that on the tailgate side. Besides, Balusu et al. (2004) and Guo et al. (2015) found that the CH_4 purity increases with the distance away from the working face due to gas desorption from residual coal and migration from adjacent strata. Anglo American Coal and CSIRO collaborated on a CFD modelling study to comprehend the goaf gas distribution of 1.0 km and 3.0 km longwall panels (Balusu et al., 2019). They investigated various mining parameters, suggested gas drainage strategies, and recommended increasing the injection of inert gas to achieve effective inertisation of the goaf area in longer panels. Furthermore, the CFD models allowed for the detailed investigation of gas flow patterns in the longwall goaf. Some researchers (Guo et al., 2015; Qin et al., 2015; Qin et al., 2017) applied CFD modelling to simulate the goaf pressure distribution and gas flow pattern under different mining conditions, such as horizontal boreholes drainage conditions, borehole locations, the depth of goaf caved zones and fractured zones, and gas release characteristics. These modelling results also provided valuable guidance to improve borehole drainage performance. Worrall Jr (2012) and Saki (2016) have employed CFD models based on US mining layouts to analyse the sensitivity of the goaf atmosphere to various factors, including permeability distribution, gas emission rate, and face ventilation. Additionally, these CFD models were employed to enhance the design of vertical boreholes within the goaf. It is important to note that the accuracy and generalisability of Worrall and Saki’s models may be constrained due to their calibration based solely on O_2 concentrations from two boreholes.

Above investigations have laid the groundwork of simulating methane-air mixture in the goaf under the impact of vertical boreholes gas drainage. However, previous studies have not incorporate a sufficient amount of field goaf gas drainage data as a reference for assessing goaf atmospheres. This study is based on extensive goaf gas production data collected from multiple Australian coal operations, the normal goaf gas profiles have been established in longwall goafs under intensive goaf drainage (total gas drainage capacity over 6000 l/s and borehole spacing at 50 m) in the earlier field data back analysis work (Si et al., 2021; Xiang et al., 2021; Wang et al., 2022a, 2022b). The back analysis results and the established conceptual model of goaf atmosphere (Fig. 2) indicate that, compared to the maingate side goaf, applying strong suction pressure on the tailgate side boreholes can cause oxygen to travel a greater distance along the tailgate side of the active goaf.

With the growing implementation of intensive goaf drainage design in gassy mines, a greater influx of ventilation air into the goaf is anticipated, leading to varying migration pathways under distinct mining conditions. The leaked ventilation air can react with residual coal in the goaf, accelerating coal self-heating, posing a threat to mine safety, and affecting gas drainage efficiency. Thus, it is imperative to investigate the

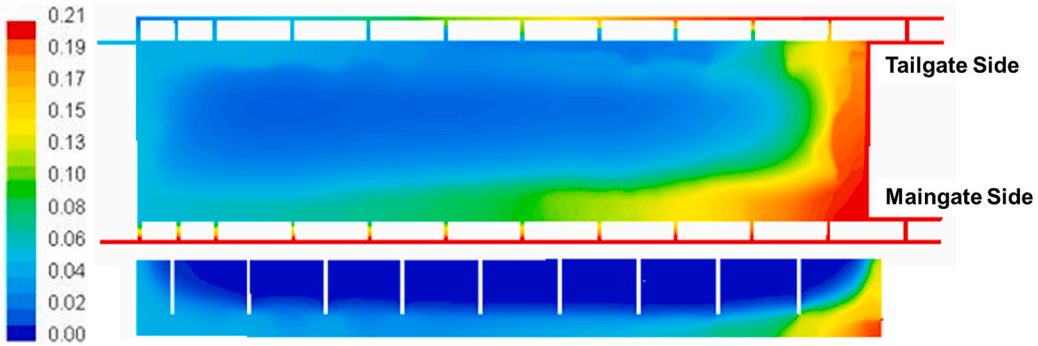

Fig. 1. O_2 distribution in the goaf under 60 m^3/s face airflow: plan view (top) and tailgate side view (bottom) (Balusu et al., 2004).

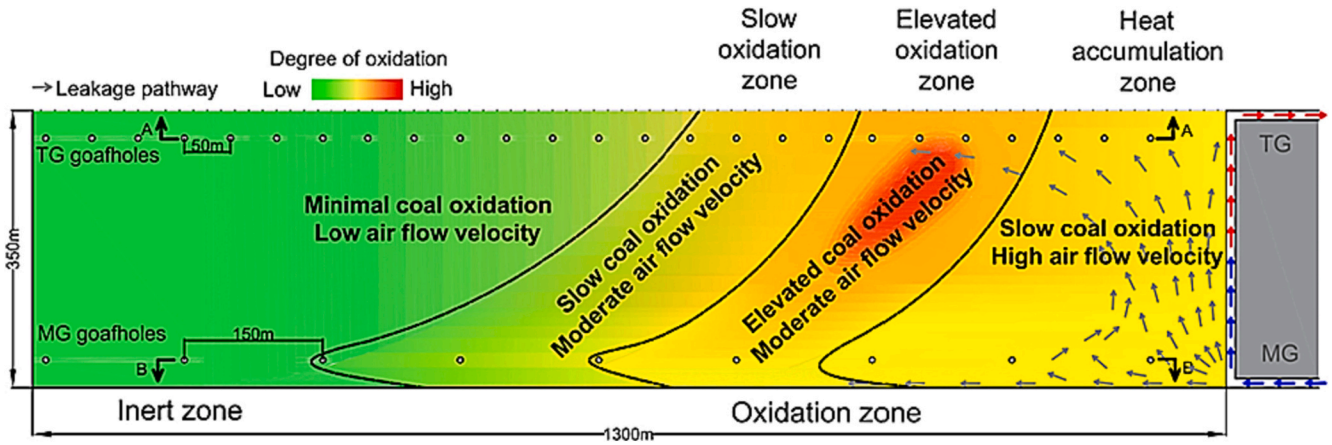

Fig. 2. The conceptual model of goaf atmosphere under intensive goaf gas drainage impact (Xiang et al., 2021).

flow pathways of leaked air from the longwall working face to the goaf under the influence of intensive goaf drainage. This paper aims to provide a comprehensive understanding of the impact of goaf gas drainage on the goaf atmosphere, especially the intensive drainage capacity currently implemented in Australian mines. It develops a goaf CFD model with eight active vertical boreholes based on the geological conditions of an underground coal mine in Australia. The model visualises gas flow patterns in the goaf under the influence of vertical boreholes, calibrated with the normal trend of goaf gas profiles obtained from extensive field data analysis (including CH_4, O_2 concentrations and gas flow rates) to ensure the accuracy of the CFD modelling simulation results. Nevertheless, previous studies have lacked an understanding of the various impacts of natural goaf characteristics with the complication of goaf gas drainage. Therefore, this study also investigates the goaf atmosphere with active vertical boreholes under different natural goaf characteristics, including goaf permeability distributions and seam gas emissions. By comparing different parameter studies, engineers can intuitively observe the impact of various natural goaf characteristics on the goaf atmosphere and make timely adjustments to the goaf gas drainage design.

2. Modelling development

2.1. Case study mine conditions and vertical boreholes implementation

In this paper, Mine A, an underground coal mine in Australia, is taken as the analysis case. A large amount of goaf drainage data collected at Mine A is used to establish the CFD model reflecting the actual field goaf atmosphere. The planned production rate for Mine A is approximately 200,000 t per week. The mining panels within Mine A operate at varying depths of cover, ranging from 250 m to 500 m, with a seam thickness of 2.8 m. Fig. 3 (a) illustrates Longwall A (LWA) within Mine A, the specific longwall panel selected for this study. LWA has a width of 350 m and extends up to 3600 m in length. Along the tailgate side of LWA, there are 74 vertical boreholes (named TG1 to TG74) spaced at approximately 50 m intervals and offset by 30 m from the tailgate side edge. Furthermore, the strata surrounding the target coal seam consist of sandstone and siltstone layers. Detailed information about these adjacent strata is depicted in Fig. 3 (b), which presents a comprehensive stratigraphic map. At Mine A, gas emissions from the coal seam typically range from 5 to 18 m^3/t (Si and Belle, 2019). Besides, the seam gas composition measured at the mine site comprises over 98% methane (Belle, 2017). As depicted in Fig. 3 (c), the vertical boreholes used in LWA follow a similar design to those described by Si and Belle (2019), with a diameter of 250 mm. The bottom of each borehole is situated approximately 10 m above the working seam. Additionally, the top portion of a borehole is typically steel cased, while the bottom 48 m of the borehole is cased with slotted pipes to allow goaf gas flow into the boreholes. These boreholes started operating at around 25 m after the longwall working face has passed by to manage the oxygen level effectively.

Comprehensive gas monitoring plans were applied to individual boreholes at LWA, including handheld gas monitors, telemetric gas sensors, and bag sample testing. The gas extracted at the wellhead of each borehole is usually sampled and measured multiple times per day by handheld instruments, which are used to measure different gas concentrations (e.g., CH_4, O_2, CO, and CO_2) from all operating boreholes in the entire production period. Moreover, the pumping systems used in Mine A were equipped with manometers to measure static pressure and differential pressure in each borehole. The baseline study of goaf gas behaviour in LWA has been presented in detail in Si et al. (2021), Xiang et al. (2021), and Wang et al. (2022b), and thus will not be repeated

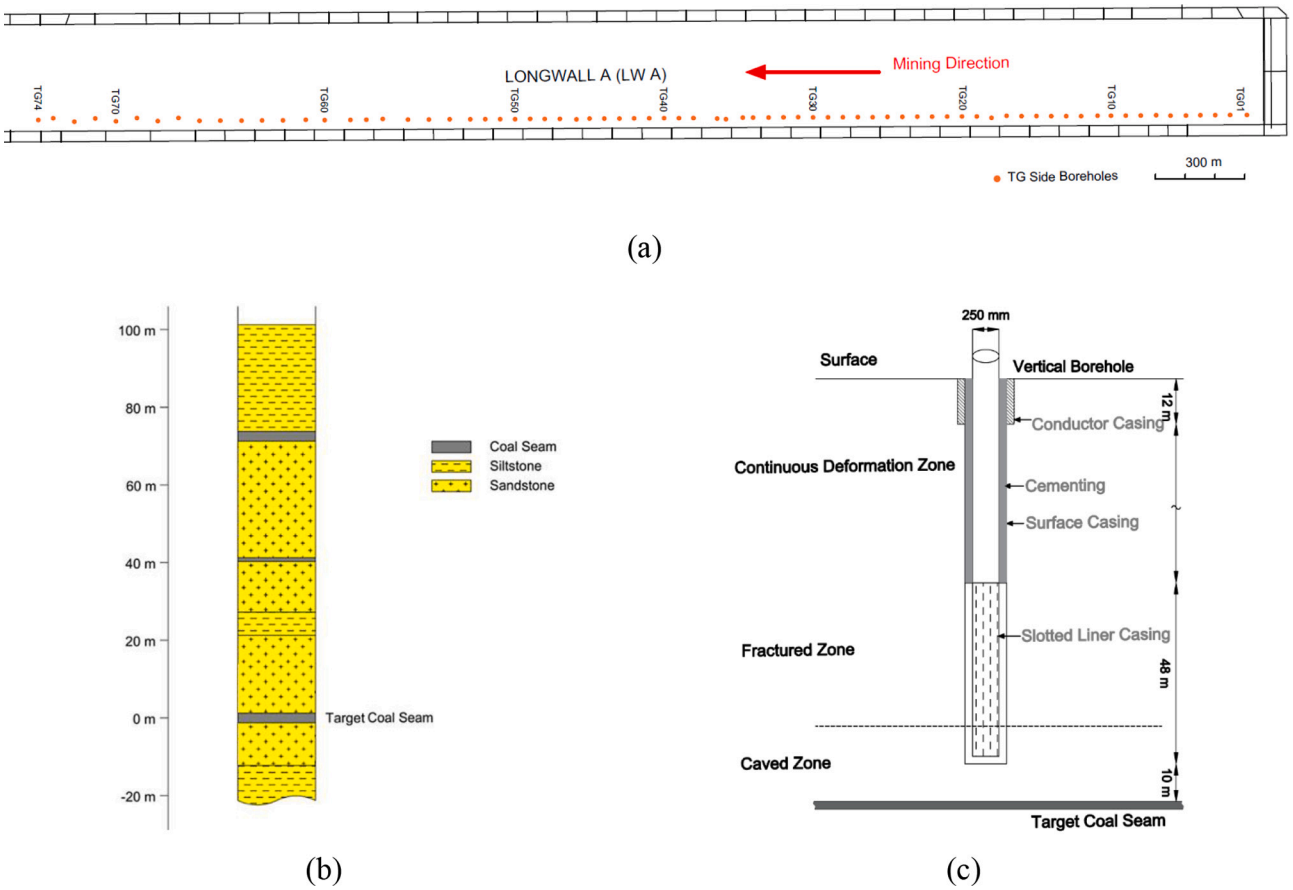

Fig. 3. (a) The schematic map of the layout of vertical boreholes, (b) stratigraphic map of the target coal seam and adjacent strata, and (c) typical vertical borehole completion plan in the study longwall panel at LWA (modified based on Wang et al. (2022a)).

here. This paper utilised the daily average values of gas concentration, gas flow rate, and suction pressure in boreholes TG1 to TG24 (during the longwall start-up stage as reported by Xiang et al., 2021) as a reference for calibrating the CFD modelling results.

2.2. Geometry definition and mesh generation

This paper used FLUENT, a mature commercial CFD software, to build the longwall goaf gas flow model to simulate the goaf atmosphere under the impact of operating vertical boreholes. The longwall goaf CFD model can be developed in the following three steps: pre-processing, solving, and post-processing. Pre-processing is the first step in

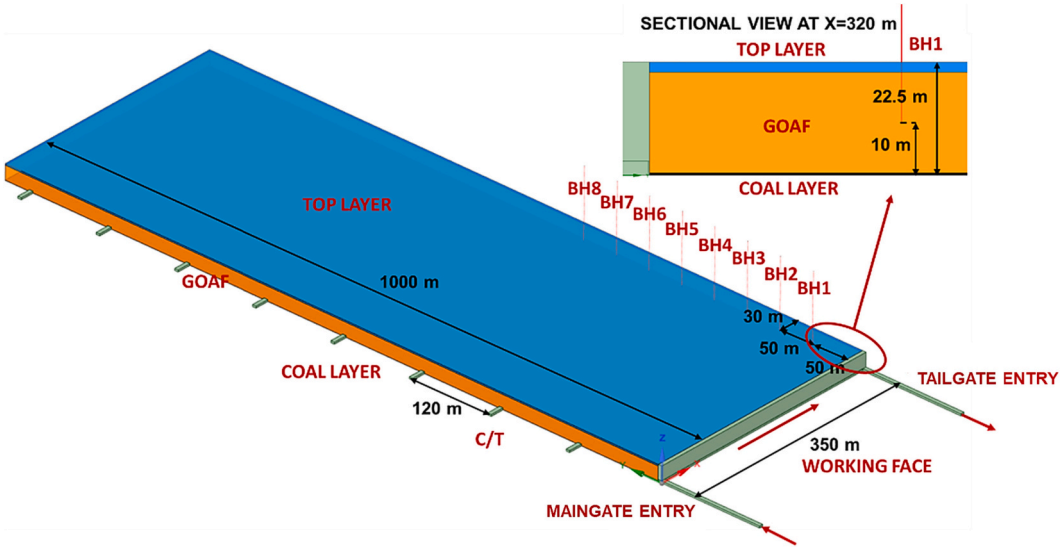

Fig. 4. Goaf geometry model developed in ANSYS FLUENT.

developing and analysing the CFD model, and it involves producing simplified geometries that can represent the field condition. The appropriate mesh is then constructed and applied to various calculation grids. After the mesh is built, the fluid parameters and physical properties are defined in FLUENT, as well as the boundary conditions, initial conditions, and solution methods. Finally, the iterative algorithm is implemented to achieve the desired convergence and accurate simulation results. The final step in the CFD model analysis is post-processing. The post-processing results will be presented in Section 3 through different types of visualisations, such as species distribution contours, goaf gas profiles, and airflow vector maps.

According to the geometry conditions of LWA and the U-type ventilation applied, a simplified goaf geometry model was built in the ANSYS package SpaceClaim, as illustrated in Fig. 4. Worrall Jr (2012) proposed that building the whole longwall panel for the progressively mined goaf is unnecessary because the results do not change after a certain length. As a result, the length of the geometry model has been reduced to 1000 m to shorten the calculation time, which is also supported by similar studies from CSIRO. Moreover, the height of this goaf geometry model is approximately 20 m, a dimension based on industry experience, which generally encompasses the depth of the goaf caved zone. The geometry model consists of three layers, as depicted in Fig. 4: the top layer (blue zone), the goaf layer (orange zone), and the bottom coal layer (black zone). More specific dimensional information on each section of the geometry model can be found in Table 1. The maingate entry is the only entrance for fresh air, which flows through the working face and then returns from the tailgate entry. In this geometry model, there are a total of eight vertical boreholes from the surface with 250 mm diameter labelled as BH1 to BH8 based on the distance from the face. BH1 is 50 m from the working face, and the rest of the boreholes have a 50 m spacing from each other. In addition, the cut-throughs (C/T) on the maingate side are 120 m apart from one another.

After establishing the geometry model, the ANSYS meshing module can be used to divide the entire geometry model into numerous grids. The number of grids in the mesh determines the accuracy of the CFD modelling results. The greater the number of grids, the greater the accuracy of the results. However, the increase in the grid number is restricted by the hardware and requires more calculation time. To balance the accuracy of calculation results and the efficiency of the CFD modelling, this model performs a mesh sensitivity analysis. This mesh sensitivity analysis is achieved by monitoring solution changes as the mesh is refined until accurate results are attained. In this paper, all components of the geometry model are meshed using the cut-cell approach with variable sizing controls to create hexahedral cells. The final mesh model comprises approximately 12 million cells, with specific mesh settings detailed in Table 1. In general, a fine grid is chosen in regions if there are significant variances in model components, whereas a coarser grid is used where the differences are minor. Consequently, this model is discretised using non-uniform grids, as specified in Table 1. As illustrated in Fig. 5, the goaf zone was combined with the fine mesh (1.5 m) near the working face and the coarse mesh (5 m) further away. Besides, all boreholes assigned a mesh size of 0.05 m, with five inflation layers featuring a growth rate of 1.2 to ensure a smooth connection between the boreholes and the goaf zone. After the meshing has been completed, the initial quality assessment of the mesh can be conducted. This mesh model achieved an average orthogonal quality of 0.97203, falling within the excellent range of 0.95 to 1. Additionally, the average skewness of the model is 0.01226, also within the excellent mesh range of 0.0 to 0.25. Then the mesh model was imported into FLUENT to be solved.

Table 1
Geometry model settings and mesh settings.

Geometry settings (width * length * height)	Mesh settings
Top layer (350 m * 1000 m * 2 m, blue zone)	1.5 m (0–450 m from the working face) & 5 m (450–1000 m from the working face)
Goaf layer (350 m * 1000 m * 20 m, orange zone)	1.5 m (0–450 m from the working face) & 5 m (450–1000 m from the working face)
Bottom coal layer (350 m * 1000 m * 0.5 m, black zone)	0.5 m
Working Face (350 m * 5.4 m * 2.8 m)	1.5 m
Working Face - Maingate entry (5.4 m * 100 m * 2.8 m)	5 m
Working Face - Tailgate entry (5.4 m * 100 m * 2.8 m)	5 m
Vertical boreholes (Φ 250 mm * 250 m, BH1 to BH8)	0.05 m

2.3. Solving methods and boundary conditions

FLUENT provides a variety of solvers for fluid flow modelling. The pressure-based solver was utilised in this study. This method calculates the pressure throughout the model using the mass and momentum conservation equations (Eqs. 1 to 3) and then extracts the density from the pressure field using the equation of state (Eq. 4) (ANSYS Inc, 2020). For the goaf CFD model, an absolute velocity formulation is recommended due to the low-speed flow in the goaf zone, and the model was assumed to be a steady-state simulation.

The conservation of mass:

$$\frac{\partial \rho}{\partial t} + \overrightarrow{\nabla} \bullet \rho \overrightarrow{v} = 0 \tag{1}$$

where ρ is the fluid density (kg/m^3); t is the time (s); $\overrightarrow{v}$ is the velocity vector (m/s).

The conservation of momentum:

$$\frac{\partial(\rho \overrightarrow{v})}{\partial t} + \overrightarrow{\nabla} \bullet (\rho \overrightarrow{v} \overrightarrow{v}) = \overrightarrow{\nabla} \bullet p + \overrightarrow{\nabla} \bullet \overrightarrow{\overrightarrow{\tau}} + \rho \overrightarrow{b} \tag{2}$$

where p is the static pressure (Pa); $\overrightarrow{b}$ is the body force, $\overrightarrow{\overrightarrow{\tau}}$ is the viscous stress tensor (Newton) in the following Eq. 3 for a Newtonian fluid.

$$\overrightarrow{\overrightarrow{\tau}} = \mu\left(\overrightarrow{\nabla} \overrightarrow{v} + \left(\overrightarrow{\nabla} \overrightarrow{v}\right)^T\right) - \frac{2}{3}\mu\left(\overrightarrow{\nabla} \overrightarrow{v}\right) \overrightarrow{\overrightarrow{I}} \tag{3}$$

$$p = \frac{nRT}{V} \tag{4}$$

where n is the number of moles of an ideal gas; R is the ideal gas constant ($8.314\ J\ K^{-1} mol^{-1}$); T is the temperature (K); V is the volume (m^3).

Furthermore, this model consisted of free-flow domains (the maingate entry, tailgate entry and working face) and porous media domains (the top layer, goaf and coal layer). In the free flow domain, the airflow was assumed to be completely turbulent, and the Standard k-ε model was set here with the standard wall function. The laminar flow zone option is enabled in the goaf and coal layer to suppress the turbulent viscosity of the fluid in the porous media domain. For the goaf and coal layer zone, viscous resistance (inverse of permeability) and porosity were defined by a User-Defined Function (UDF) code. This code is based on a fitting result derived from the theoretical resistance model, which was obtained through back analysis results as presented in earlier work (Wang et al., 2022a, 2022b) and previously reported goaf permeability values (Esterhuizen and Karacan, 2007; Karacan, 2009; Marts et al., 2014; Zhang et al., 2016, Zhang et al., 2019a, 2019b). Fig. 6 (a) illustrates the goaf porosity contour on the horizontal plane applied in this goaf CFD modelling. Additionally, the permeability change in the goaf caved zone was estimated using the Kozeny-Carmen equation (Eq. 5). In this model, the permeability change was assumed to be equivalent along the goaf maingate and tailgate sides, with the seam fully compacted at approximately 75 m behind the working face. This resulted in a permeability range from1e-4 to 1e-9 m^2 in the horizontal plane view, as

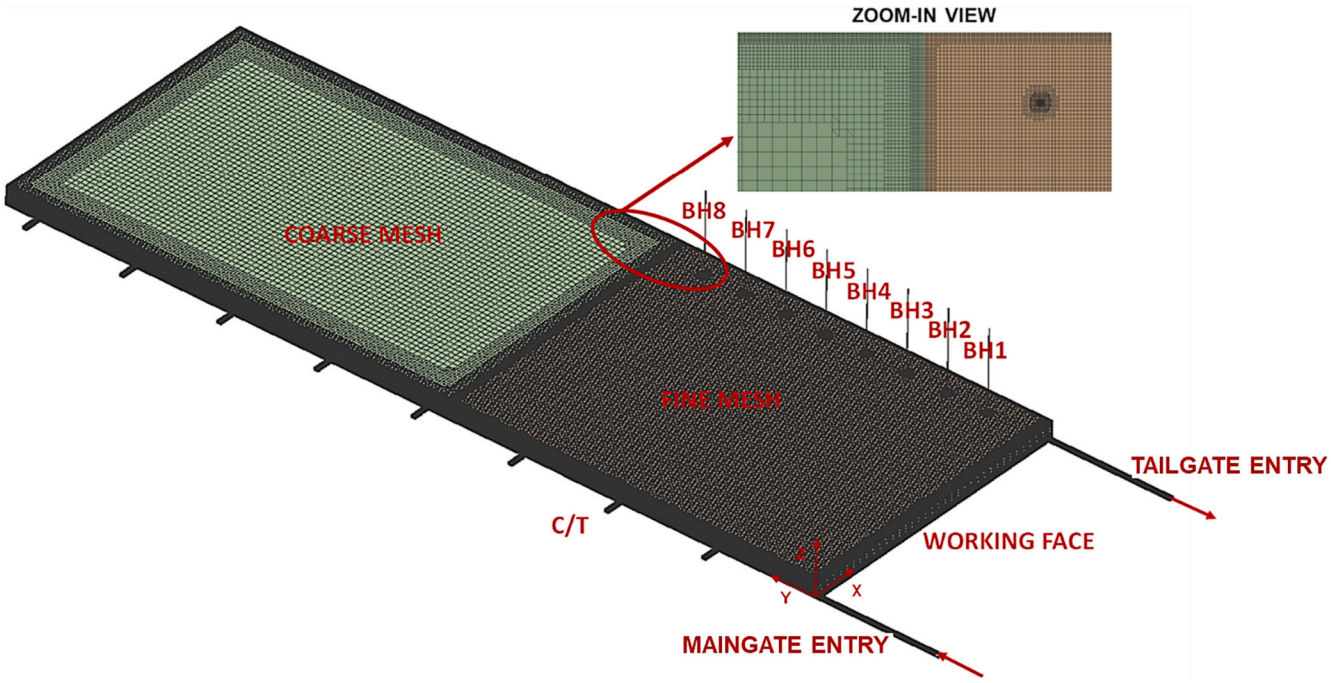

Fig. 5. Goaf mesh model developed in ANSYS FLUENT.

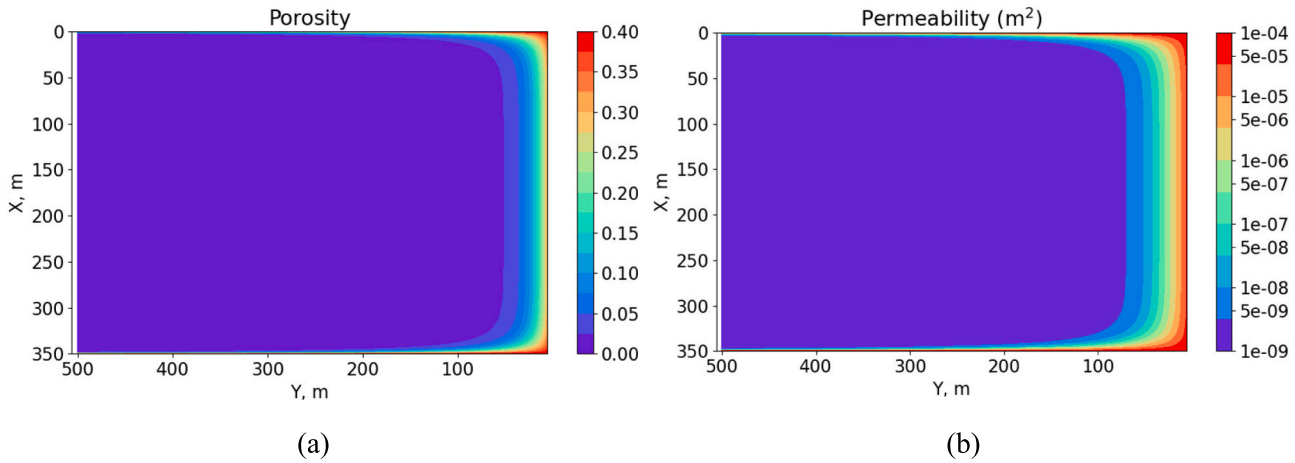

Fig. 6. (a) The goaf porosity distribution and (b) the goaf permeability distribution in the horizontal plan view.

shown in Fig. 6 (b). Furthermore, this paper assumed that the porosity and permeability of the goaf caved zone are distributed symmetrically along the central lines of x = 175 and y = 500 m. Given that the depth of the goaf caved zone in this model is about 20 m, it is assumed that porosity and permeability along the *Z*-axis remain constant over this relatively short vertical distance. The impact of the permeability distribution on the goaf atmosphere will be discussed in detail in Section 4.1.

$$k = \frac{\varphi^3 d^2}{150(1-\varphi)^2} \tag{5}$$

where k is the permeability (m^2); φ is the porosity; d is the mean particle diameter of the porous medium, equal to 0.3 m in this case (Yuan et al., 2006; Karacan, 2010; Zhang et al., 2019a, 2019b).

In the boundary condition settings, the inlet and outlet properties can be specified. This model has two inlets: one for ventilation air and one for gas emissions. The maingate entry, as the sole source of air leakage for the longwall working face, is configured as a velocity inlet. This ventilation inlet has a velocity magnitude of 3.97 m/s and provides 60 m^3/s of air to the longwall working face. Taking into account the molar fraction of the gas mixture in the atmosphere, the leaked air from the ventilation inlet (maingate entry) contains 20.93% O_2. For the gas emission inlet, considering that the target coal seam has nearly been completely mined, the top layer is simplified as the exclusive source of gas emission in this model. As depicted in Fig. 7, each blue triangle represents the cumulative CH_4 flow rate across all operating boreholes at a particular distance from the face. The solid blue line illustrates the trend of the mean cumulative CH_4 flow rates, calculated as a rolling average over 20 m, along the direction of the working face. This graph clearly indicates that the maximum cumulative CH_4 flow rate from all operating boreholes can reach approximately 5800 l/s. In addition to the gas extracted through vertical boreholes, there exists a trace amount of gas (less than 2%, according to the QLD mine safety threshold) that could escape from the tailgate entry. Given that the total ventilation airflow rate at the maingate entry is ~60 m^3/s, the CH_4 flow rate leaking from the tailgate entry would not exceed 1200 l/s based on the 2% statutory CH_4 limit (60 m^3/s × 2% × 1000 = 1200 l/s). Consequently,

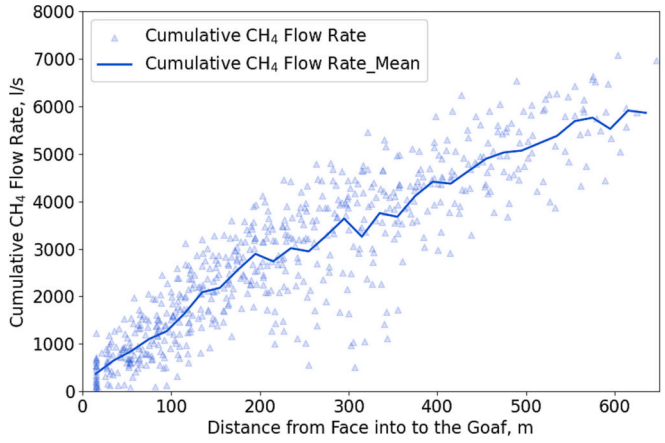

Fig. 7. Cumulative CH_4 flow rate from drained vertical boreholes at LWA.

the initial assumption in this paper was that the total gas emission uniformly emitted to the goaf from the top layer at a rate of 7000 l/s. Based on the gas reservoir condition of Mine A, the purity of the gas emission in this CFD model is assumed to be 100% CH_4 to simplify the calculation. Moreover, it is important to note that gas emission is not constant along the length of the in-situ longwall panel, as indicated by previous research on gas emission storage (Lunarzewski, 1998; Guo et al., 2008; Qu et al., 2022). A comprehensive discussion regarding the impact of varying gas emission rate trends and magnitudes on the goaf atmosphere, considering the presence of operating boreholes, will be presented in Section 4.2. In this CFD model, the gas mixture within the goaf was extracted through eight active vertical boreholes by applying suction pressure at their surfaces. According to the field data provided by LWA (Fig. 8), the suction pressure applied to most boreholes in the operation period ranged from 4 kPa to 10 kPa. As a result, a constant mean pressure of −6.5 kPa was applied to the top of eight boreholes.

3. Modelling results and field data comparsion

Once the CFD model had been established with the instructions laid out in Section 2, the FLUENT solver converges after approximately 20,000 iterations, reaching equilibrium with residuals below 1e-3. To ensure the accuracy of the goaf CFD model, a large amount of field data collected from the LWA tailgate side boreholes (start-up stage: TG1 to TG24) was compared with the CFD modelling results. The CFD modelling results will be analysed in detail in the following sections to gain a comprehensive understanding of the goaf atmosphere and gas flow patterns, particularly under the impact of goaf gas drainage via these

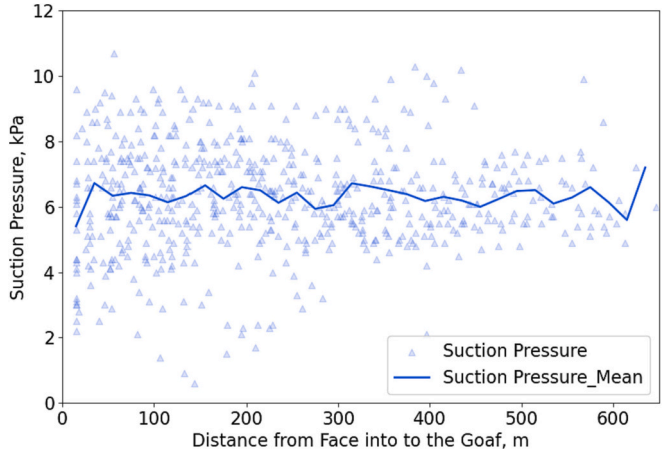

Fig. 8. Suction pressure applied on the top of vertical boreholes at LWA.

vertical boreholes.

3.1. Goaf CH_4 distributions

The CH_4 distributions of CFD modelling results are displayed in Fig. 9 and Fig. 10 under the drainage impact of eight vertical boreholes. There is a 3D view contour of various cut-planes (Fig. 9 (a)), including a horizontal cut-plane at the depth of 10 m above the target coal seam (i.e., the borehole completion depth), a vertical cut-plane at 30 m away from the tailgate side edge (i.e., boreholes vertical location), and another vertical cut-plane at 30 m away from the maingate side edge for comparisons purposes. It can be clearly seen that the CH_4 level is quite low near the working face due to the sweep of ventilation air from the working face and slowly rising in the deeper goaf. From the zoom-in contour of the vertical cut-plane taken at 30 m away from the tailgate side and another one at 30 m away from the maingate side (Fig. 9 (b)), the CH_4 concentration in the goaf varies at different depths and locations. In both two vertical plane zoom-in views, gas emissions from the top layer constantly infiltrate the goaf, leading to a higher CH_4 concentration near the roof. Meanwhile, the ventilation air dilutes the goaf gas as it moves away from the roof, resulting in lower CH_4 concentrations. In comparison to the maingate side, the tailgate side allows diluted gas to enter the vertical borehole through the slotted casing due to the application of suction pressure on the borehole. Moreover, the low CH_4 zone (less than 20%) on the tailgate side extends to a position farther from the bottom of the goaf.

Furthermore, Fig. 10 displays the CH_4 contour at different horizontal cut-planes (at 5 m, 10 m, 15 m, and 20 m above the seam height). The graph demonstrates that, as moving up into the goaf, CH_4 rises quickly on the maingate side, and the size of the low CH_4 zone gradually decreases behind the working face. In contrast to the maingate side, the tailgate side has much lower CH_4 since the goaf gas drainage has drawn a large amount of air into this side goaf. This phenomenon is particularly noticeable at 15 m and 20 m above the seam (Fig. 10 (c) and (d)), where low CH_4 levels are maintained for a long distance after passing through the tailgate corner. Additionally, it shows that the CH_4 concentration at the tailgate goaf side gradually increases with the goaf height, which may be due to the progressive proximity to the top layer (gas emission source). In the plan view at a distance of 20 m from the seam (Fig. 10 (d)), the CH_4 concentration behind BH6 on the tailgate side (300 m away from the working face) exceeds 90%, constituting the predominant gas within the goaf.

To further understand the distribution of CH_4 concentration in goaf under the impact of intensive goaf gas drainage, Fig. 11 depicts the CH_4 profiles along the dashed line of the tailgate side (as shown in Fig. 10) at various heights of horizontal cut-planes. In cases where the cut-planes are situated farther away from the gas source at the top layer (e.g., at 5 m and 10 m of the tailgate side goaf) in Fig. 11, the CH_4 profile along the tailgate side goaf remains at a lower level due to the dilution effect of the air from the working face. It then rapidly escalates to approximately 100% after reaching a distance of about 400 m. Apart from the CH_4 profiles at 5 m and 10 m, the CH_4 profiles at other depths within the tailgate side goaf gradually increases to around 100%. When comparing the CH_4 profiles at different depths on the tailgate side goaf, the CH_4 concentration increases as the horizontal cut-planes get closer to the top layer, which is consistent with the CH_4 contours in Fig. 10. Besides, the CH_4 profile along the maingate side goaf, located 10 m above the seam, is represented by the black dashed line in Fig. 11. This profile displays a slower increase compared to the tailgate side, primarily due to the absence of borehole drainage. The black dots in Fig. 11 represent the simulated CH_4 purity obtained from eight drained boreholes in this CFD model. In BH1, the CH_4 concentration is approximately 20%, and as the distance from the working face increases, it progressively rises to around 80% in BH8. Furthermore, the CH_4 concentration at the tailgate entry from this CFD model is approximately 1.4%. It is consistent with the findings of Belle (2014) that CH_4 concentrations at the tailgate of the

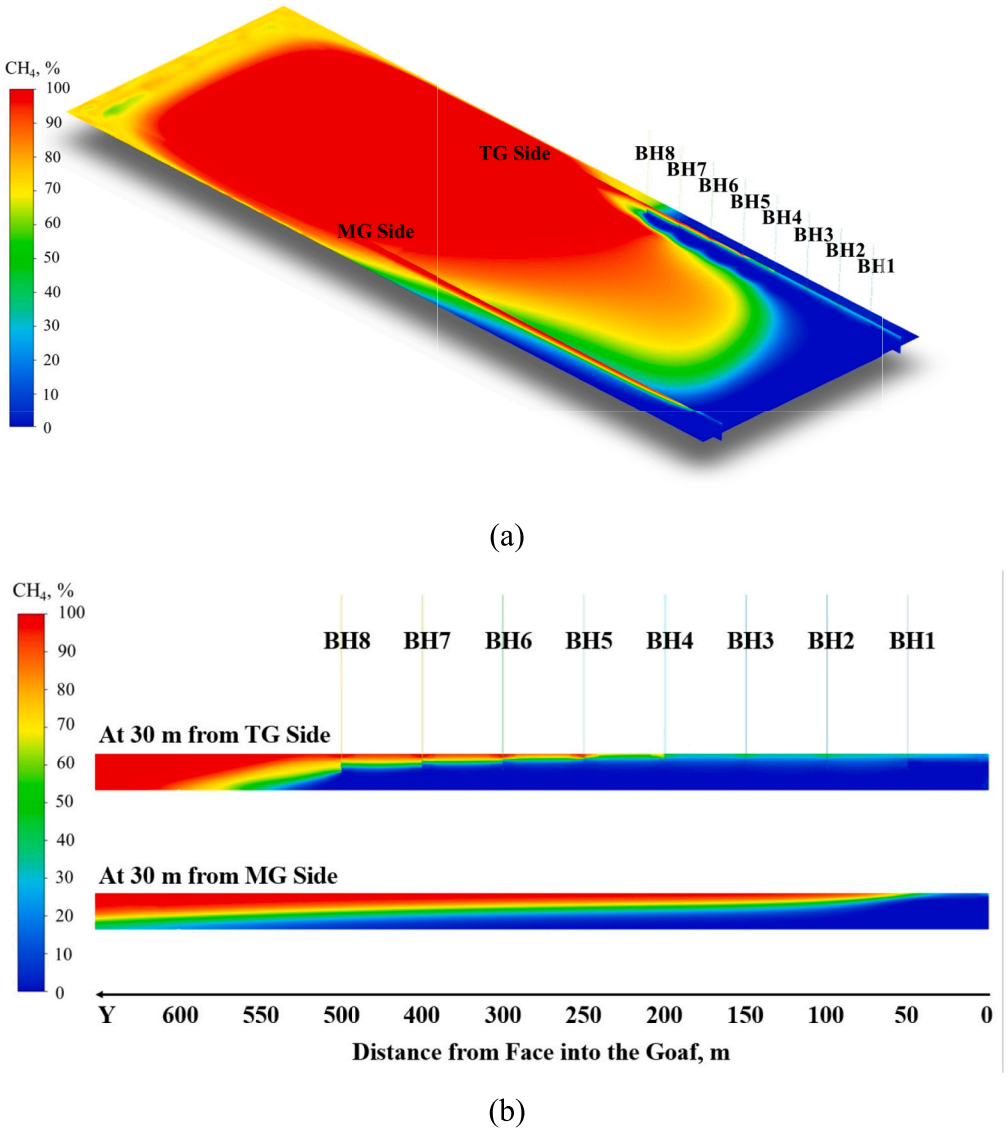

Fig. 9. CH_4 contour (a) in 3D view and (b) zoom-in view of the vertical cut-plane at 30 m offset from the tailgate and maingate sides edges.

Australian longwall panel vary from 0.5% to 1.5%.

The gas concentrations extracted from eight boreholes in the CFD model can be compared with the gas drainage data obtained from the LWA tailgate side boreholes. The CH_4 concentrations extracted from the tailgate side boreholes (TG1 to TG24) at LWA are presented in Fig. 12, where each blue triangular on the plot represents the CH_4 concentration measured at the borehole located at a certain distance from the longwall working face. The solid blue line in Fig. 12 represents the rolling median (with 20 m spacing) of the gas concentrations, while the solid orange lines represent the Q1 (25%) and Q3 (75%) quartiles of the CH_4 concentration. From this graph, it can be observed that the CH_4 content extracted from boreholes closer to the working face displays a substantial range of variation, spanning from 20% to 90%. Additionally, Fig. 12 clearly illustrates that the median value of CH_4 concentration obtained from the field goaf gas drainage data slowly decreases to 300 m back into the goaf, followed by a progressive increase to 70%. The CH_4 concentration obtained from eight boreholes in this CFD model exhibits a consistent range of variation with the value derived from on-site measurements. However, there is a discernible trend of increasing CH_4 concentration from BH1 to BH8, which reflects a particular scenario. This trend might be attributed to the assumption in the CFD model that gas emissions from the top layer uniformly enter into the goaf. The distinct impacts of different gas emissions on the goaf atmosphere under the influence of vertical boreholes will be discussed in Section 4.1.

3.2. *Goaf O_2 distributions*

Similarly, Fig. 13 (a) below presents a 3D view depicting the O_2 distribution in the goaf with eight active vertical boreholes. It is clear that the implementation of intensive goaf gas drainage results in the presence of an O_2-rich zone (greater than 5%) not only within the area behind the working face, but also extending into the tailgate side goaf. Moreover, the concentration of O_2 on the maingate side is lower compared to that on the tailgate side. Examining the 2D zoomed-in view of the O_2 contour at a distance of 30 m offset from the tailgate side edge (top part of Fig. 13 (b)), it becomes apparent that the O_2-rich zone on the tailgate side goaf extends from the lower goaf towards the top layer, almost covering the entire depth of the caved zone near the face. Additionally, the zoom-in view of the O_2 contour on both the tailgate and maingate sides reveal a noticeable decrease in O_2 content as the distance from the bottom of the goaf increases. This observation is further supported by the subsequent O_2 contour (Fig. 14) conducted across different horizontal cut-planes. Furthermore, this suggests that the highest O_2 concentration is situated at the mining level in this

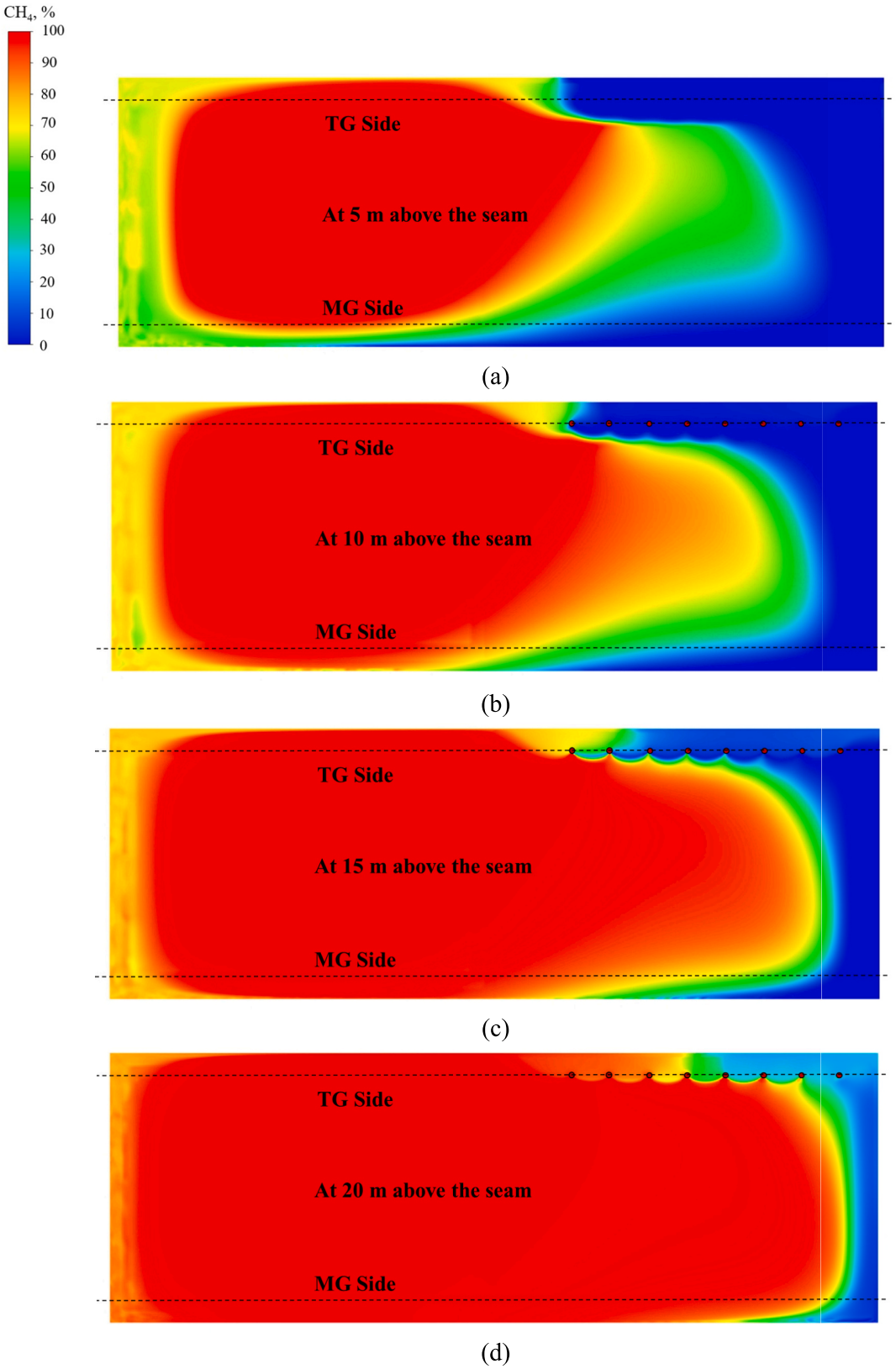

Fig. 10. CH_4 contour at different horizontal cut-planes: (a) 5 m, (b) 10 m, (c) 15 m and (d) 20 m above the seam.

specific scenario.

To further inspect the O_2 ingress zone on the tailgate side goaf at different elevations, the horizontal cut-planes of the O_2 contour at different heights above the seam (at 5 m, at 10 m, at 15 m, and at 20 m) are shown in Fig. 14. It can be observed that the size of the O_2-rich zone near the working face is smaller as moving higher into the goaf. This upward migration of O_2 from the face to the upper goaf sections appears to adopt a 'pyramid' pattern. Moreover, the travel distance of high-

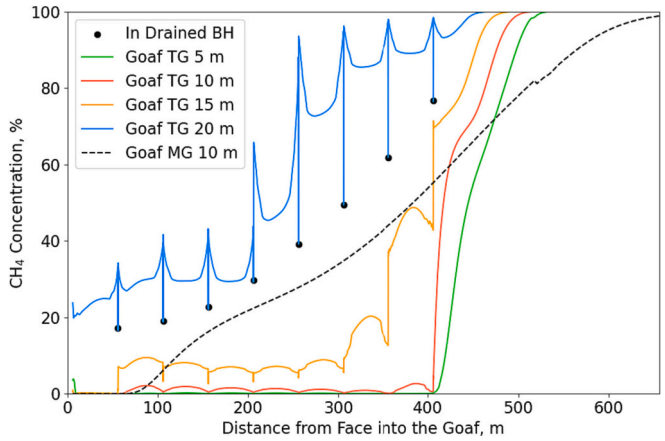

Fig. 11. CH_4 concentrations in the goaf and drained boreholes from CFD modelling results.

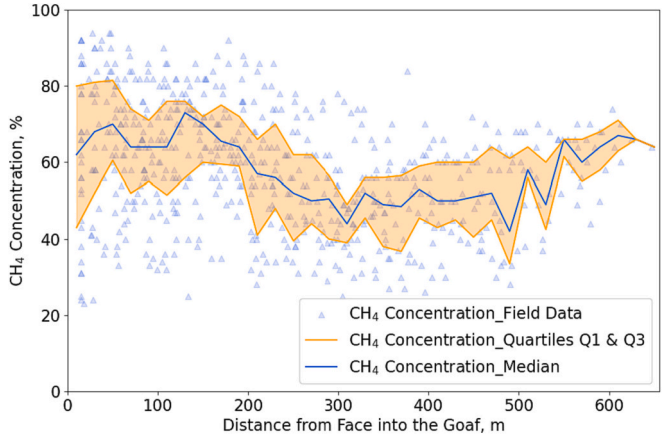

Fig. 12. CH_4 concentrations from the field goaf gas drainage data.

purity O_2 experiences a rapid reduction as the height increases on the maingate side. However, for the tailgate side goaf, the O_2 level is reported to be much higher due to the strong suction pressure applied to these boreholes. As can be seen from Fig. 14 (d), BH1 to BH6 can pull over 5% of O_2 up to 20 m above the seam at a distance of 300 m from the face. This is attributed to the greater distance of BH7 and BH8 from the face, and the leaking air was preferentially extracted from the closer boreholes.

The O_2 profile along the dashed line on the tailgate side goaf (Fig. 14) is presented in Fig. 15, where solid lines of different colours illustrate the O_2 profiles corresponding to different goaf heights. Furthermore, the black dots in Fig. 15 represent the O_2 concentrations drained in eight vertical boreholes from the CFD model, with levels gradually decreasing from 17.5% in BH1 to 5% in BH8. As Fig. 15 illustrates, for both the 5 m and 10 m cases, the O_2 concentration within the tailgate side goaf remains at a high level (almost 21%) in the first 400 m towards the face, sharply declining to an extremely low after that. However, the O_2 profiles in the maingate side goaf, situated 10 m above the seam and marked by the black dashed line in Fig. 15, initially sustain a high-purity O_2 content within the first 100 m. Following this, a more gradual decline is observed in comparison to the tailgate side goaf, reaching an extremely low level at approximately 650 m. Additionally, it can be observed that when the height is greater than 10 m, the O_2 concentration in the tailgate side goaf decreases obviously as the goaf height increases. This is reasonable as boreholes would preferentially drain CH_4 emitted from the top layer. Consequently, this also explains why the O_2 concentration in the goaf close to the borehole bottom (at 10 m above the seam, represented by the yellow solid line) is higher than that in the drained boreholes (denoted by black dots in Fig. 15).

Similar to Fig. 12, the O_2 concentrations from field production data are displayed in Fig. 16. The graph illustrates a gradual decline in the median O_2 levels from the vertical boreholes at the site, decreasing from an initial value of ~9% to ~2% at 650 m from the face. However, the O_2 concentrations fluctuate over a wide range within 100 m close to the face, with many of the field data points showing very low O_2 levels (less than 5%) or high O_2 levels (more than 12%). Consistent with the trend observed in the field data, the O_2 concentration in eight operating boreholes in the CFD modelling results also demonstrates a decreasing trend. Moreover, the O_2 concentration in the goaf and drained boreholes is affected by the natural characteristics of the goaf, including the goaf permeability distribution and gas emission rate. The influence of these factors on the goaf atmosphere will be discussed in Section 4.

3.3. *Goaf gas flow patterns*

In addition to understanding the goaf atmosphere under the influence of goaf gas drainage, it is also important to understand the airflow dynamics around the operating vertical boreholes. Fig. 17 shows the zoom-in view of airflow vectors near the working face area at different goaf heights and how the ventilation air migrates from the face to these boreholes. Besides, the vector arrows are coloured by O_2 concentration, which can indicate the pathways for airflow in the goaf. As depicted in Fig. 18 (b, showing the air vector at the borehole completion depth), ventilation air enters through the maingate inlet and proceeds to traverse along the maingate side edge before following the working face towards the tailgate side boreholes. This finding further validates the speculated airflow pathways in the earlier conceptual model (Fig. 2) based on back analysis results (Xiang et al., 2021). For boreholes situated near the working face (BH1 to BH3), the air within the drainage boreholes encompasses not only the air directly from the working face but also the air that travels along the tailgate side goaf edge via high-permeability channels. As the borehole progressively moves away from the working face and the compaction level in the goaf centre increases, it becomes challenging for leaked air to flow directly from the maingate side to the borehole. Consequently, the air within these boreholes primarily flows in from the high-permeability channel on the tailgate side edge. Moreover, when the borehole is considerably distant from the working face, such as BH8 in this case, it becomes evident that a portion of the air leakage circulates back into the borehole along the goaf edge due to the intensive goaf gas drainage. Therefore, a monotonical decrease of O_2 and an increase of CH_4 would be observed at tailgate side boreholes in Fig. 11 and Fig. 15. The sweep of ventilation air would result in significant high O_2 concentration and low CH_4 close to the longwall face, and this effect diminishes as moving into the deep goaf.

Furthermore, Fig. 18 (a) shows the plan view of the whole vector field in the goaf (at 10 m above the seam) with the application of eight vertical boreholes. The vector arrows are coloured by velocity magnitude, and the contour plot reflecting the velocity magnitude is also shown in Fig. 18 (b). Except for the area near the working face, the flow velocity in the goaf is observed to be greater near the borehole locations and the tailgate side edge, as compared to other areas in the goaf. As the gas flows from the relatively wide and large void space of the goaf into a thinner borehole, there will be a large increase in the velocity at the borehole location to ensure the conservation of mass. Additionally, the gas mixture in the goaf will change from laminar flow to turbulent flow near the borehole location. Moreover, the uncaved or unconsolidated goaf at the tailgate side edge provides a fast flow channel for leaked air. Thus, the ventilation air from the maingate side travels along the working face and tailgate side edge and is finally extracted by the boreholes. Based on the CFD modelling results in this paper, the existence of the high-permeability air leakage pathway from the tailgate corner via the goaf edge to goaf boreholes at different locations may be

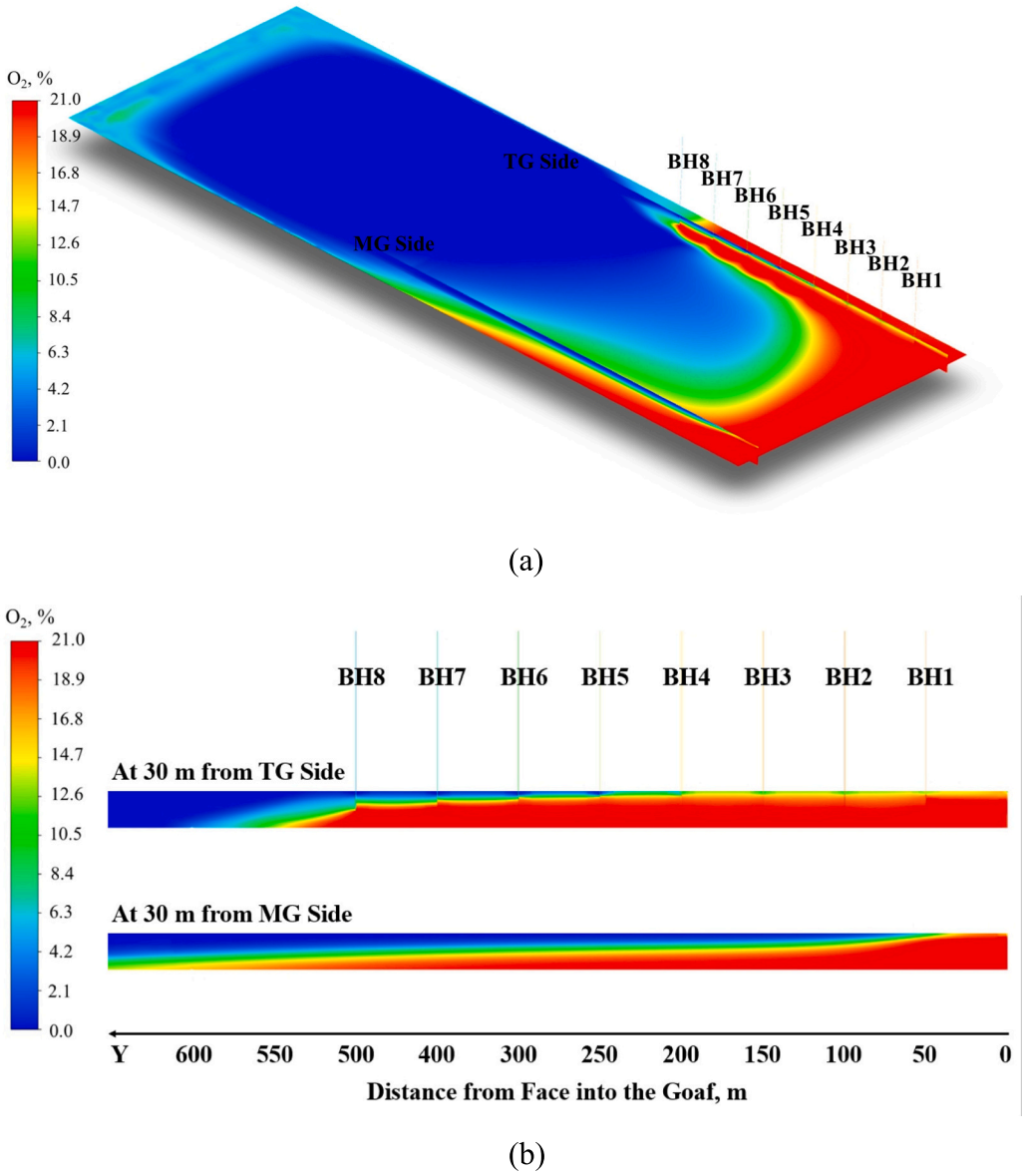

Fig. 13. O_2 contour (a) in 3D view and (b) zoom-in view of the vertical cut-plane at 30 m offset from the tailgate and maingate sides edges.

the main reason for O_2 ingress into the tailgate side goaf.

4. Discussions

4.1. Impact of goaf permeability distribution

In Section 2.3, it is proposed that the goaf permeability in this CFD model is determined by combining the theoretical goaf resistance model proposed in earlier back-analysis results with previous goaf permeability studies (Esterhuizen and Karacan, 2007; Karacan, 2009; Ren et al., 2011; Marts et al., 2014; Zhang et al., 2016, 2019a, 2019b). By utilising the theoretical resistance model (Wang et al., 2022a, 2022b), it is possible to calculate the goaf resistance for the case study longwall panel. The results from LWA indicate a sharp increase in resistance after the working face, reaching a peak at 50–100 m back into the goaf and then remaining stable. Since goaf permeability is inversely related to goaf resistance, the permeability along the tailgate side dashed line at the borehole completion depth (Fig. 10 (b) and Fig. 14 (b)) can be estimated. Moreover, the overlying strata would fully compact within 50–100 m from the face. Therefore, this paper adopts an 'O-shaped' permeability distribution for the goaf, with a magnitude ranging from 1e-4 to 1e-9 m^2 as illustrated in Fig. 6. This distribution corresponds to the original permeability input for the subsequent analysis.

Since the distribution of permeability affects the goaf environment, this section will analyse the effects of varying permeability conditions on the goaf atmosphere with the complication of goaf gas drainage. Fig. 19 illustrates the permeability contour at 10 m above the seam under different scenarios of goaf permeability distribution. Cases 1 and 2, depicted in Fig. 19 (a) and (b) respectively, represent distinct compaction scenarios behind the working face while maintaining a consistent permeability magnitude. Furthermore, Fig. 19 (c) and (d) display Case 3 and Case 4, respectively, wherein varying permeability ranges are achieved by manipulating the mean particle diameter (d) as described in Eq. 5. In these two cases, the distance from the fully compacted goaf to the face remains consistent with the original case. By keeping all other parameters of the CFD modelling constant, simulation results corresponding to different permeability cases can be obtained.

As shown in Fig. 20, different colours represent the CFD simulation results for various cases. The different scatter points represent the CH_4 and O_2 content of the gas mixture extracted from the borehole. Besides,

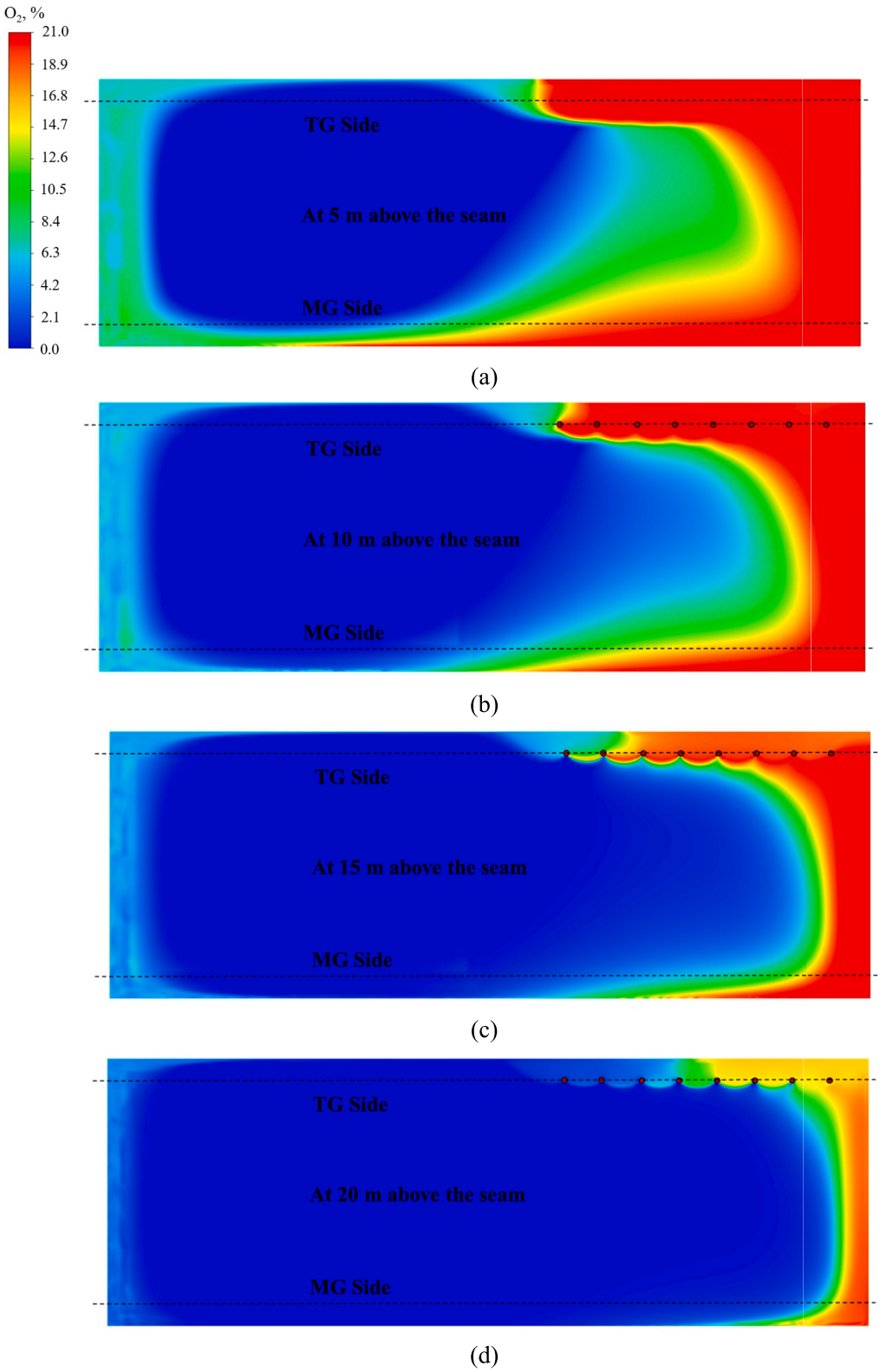

Fig. 14. O_2 contour at different horizontal cut-planes: (a) 5 m, (b) 10 m, (c) 15 m and (d) 20 m above the seam.

the solid line indicates the gas profiles at 30 m offset from the tailgate side edge, while the dashed line displays the results at 30 m offset from the maingate side edge, and specifically, they are both at 10 m above the seam. When the overburden in Case 1 collapses and compacts rapidly after the working face, the range of permeability variation remains the same as the original permeability input. As shown by the orange dashed line in Fig. 20 (c), O_2 entering from the maingate entry will travel along the maingate side goaf for a longer distance, remain at a high level, and then decrease rapidly. In this case, the air leaking from the working face can only travel up to 300 m from the face on the tailgate side, although the same suction pressure is applied at the top of the borehole on the tailgate side. After this, the O_2 profile of the tailgate side decreases

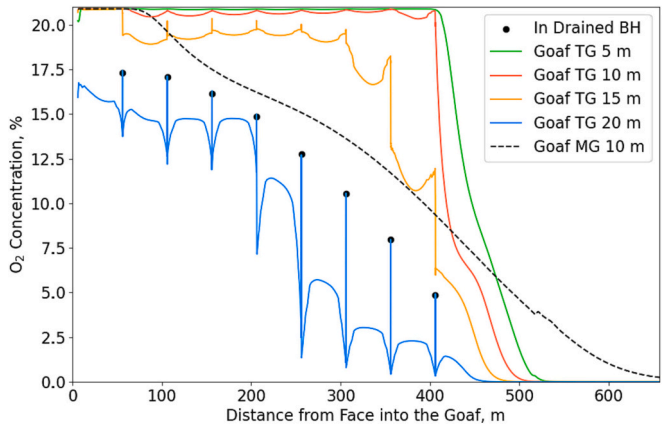

Fig. 15. O_2 concentrations in the goaf and drained boreholes from CFD modelling results.

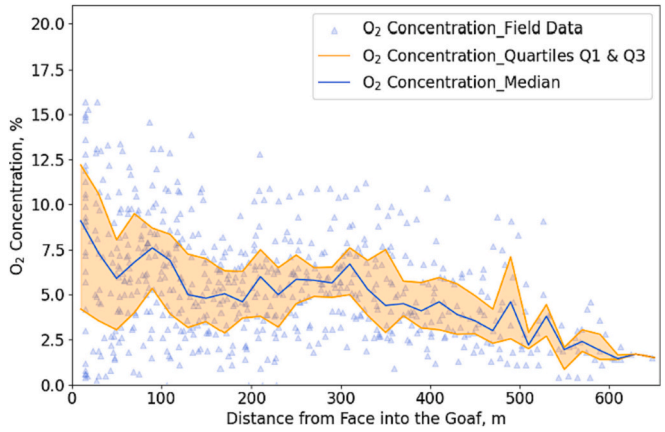

Fig. 16. O_2 concentrations from the field goaf gas drainage data.

rapidly, and the corresponding CH_4 rises rapidly due to the gas emission from the top layer. In Case 2, the goaf compaction slows down and reaches a permeability minimum at about 150 m behind the working face. Because of the increase in permeability near the working face, CH_4 is more likely to enter this area under the influence of intensive drainage from vertical boreholes. Consequently, in Case 2, the CH_4 concentration along the tailgate side goaf shows a decreasing trend, as does BH1-BH3 (Fig. 20 (a)). In contrast, an increasing trend in O_2 concentration was observed from BH1 (50 m from the face) to BH3 (150 m from the face). This trend of O_2 levels rising to a peak and then decreasing can be observed in the longwall panel adjacent to the LWA as shown in Fig. 21. Thus, the compaction degree may be one of the reasons for the large variation in O_2 concentration in the boreholes close to the working face.

To further analyse the effect of permeability magnitude on the goaf atmosphere, Case 3 shows a smaller range of goaf permeability (5e-10 m^2 to 5e-5 m^2), with an average particle diameter of 0.15 m for the goaf-porous median in this CFD model. Compared to the original case, the O_2 profile decreases slowly to 300 m after maintaining a high level at 75 m on the maingate side goaf (Fig. 20 (d)). Additionally, as the maximum permeability of the goaf edge decreases, the amount of leaked air returning to the borehole along the high permeability channel decreases, resulting in a rapid reduction in the boreholes away from the face (BH6-BH8). When the goaf permeability increased from 5e-9 m^2 to 5e-4 m^2 in Case 4, the percentage of CH_4 along the tailgate side goaf and in drained boreholes increased significantly, as depicted in Fig. 20 (b). Meanwhile, due to the enhanced permeability of the goaf, more leakage air enters the deeper goaf from the face, resulting in more O_2 and less CH_4 at the borehole completion level.

4.2. Impact of goaf gas emissions

As previously mentioned, the top layer serves as the sole source of gas emissions in this CFD model. In the original scenario, the gas emission was assumed at a rate of 7000 l/s, uniformly flowing into the goaf through the top layer. However, alterations in the distribution and magnitude of the gas emission rate directly impact the goaf atmosphere. Based on the field goaf gas drainage data, the blue triangle featured in Fig. 22 (a) denotes the daily average CH_4 flow rate at specific distances from the face. This is calculated by multiplying the total flow rate within the drained borehole by its CH_4 concentration. Simultaneously, the blue solid line represents the median CH_4 flow rate within drained boreholes, smoothed using a 20 m rolling average. It initially increases, reaching its peak value at 100 m from the face, and then decreases up to 300 m, after which it stabilises. Assuming that each borehole could extract the gas within a range of 50 m (spacing between adjacent boreholes), the fitted curve representing the gas emission rates for Case I is shown as a red dashed line in Fig. 22 (a). The gas emissions are also implemented in FLUENT using the UDF code, with a consistent value maintained in the direction parallel to the face. In Case II, Fig. 22 (b) uses blue triangles to show the CH_4 flow velocity in each drainage borehole, normalized by dividing by the distance to the previous borehole. As depicted in Fig. 22 (b), the gas emission rates set in Case II also follow a fitted curve of median values, decreasing from ~22.5 l/(s·m) to ~5.0 l/(s·m) at 350 m from the working face, and remaining constant thereafter. Furthermore, the total gas emission rate remains consistent across the original case, Case I, and Case II, which are all at 7000 l/s. This study also assesses the impact of the total gas emission magnitude on the goaf atmosphere. For example, the total gas emission decreased by half in Case III (3500 l/s) and doubled in Case IV (14,000 l/s). The boundary conditions were changed to the different gas emission inputs mentioned above while keeping other parameters constant in CFD models to obtain the corresponding simulation results.

Similar to Fig. 20, Fig. 23 shows the CFD simulation results for different gas emission scenarios, each represented by distinct colours. The total amount of gas emission in Cases I and II is the same as in the original case, but the gas emission rate is higher near the working face. As a result, the boreholes near the face in both Cases I and II show an increase in CH_4 concentration and a decrease in O_2 concentration. On the maingate side goaf, the CH_4 profile rises rapidly immediately behind the working face in Fig. 23 (a). After approximately 300 m from the working face, the gas emission rate stabilises, causing the CH_4 profile to return to the original case upward trend. However, owing to the influence of intense goaf gas drainage, CH_4 concentrations in Cases I and II remain low within the 0–400 m range on the tailgate side and then rapidly increase to 100%. As shown in Fig. 23 (c), the O_2 concentration exhibit contrasting behaviours with the CH_4 concentration. Moreover, this suggests that ventilation air from the working face is the dominant gas component in this area under the given gas emission conditions (7000 l/s).

In Case III, the total gas emissions were reduced to 3500 l/s, resulting in lower CH_4 concentrations in both the drained boreholes and the goaf compared to the original case, as shown in Fig. 23 (b). When the total gas emission increased to twice that of the original case (i.e., 14,000 l/s), a significant increase in CH_4 concentration was observed in vertical boreholes and goaf, while the O_2 concentration decreased. Furthermore, as the gas emission rate escalates to a specific value (Case IV), higher levels of CH_4 enter the goaf area near the working face due to the higher permeability of that area. Consequently, BH1 closer to the working face will extract more CH_4 and less O_2 than BH2 further away from the face. In general, the gas emission rate directly impacts the goaf atmosphere, wherein higher gas emission rates result in increased CH_4 levels within the goaf, higher CH_4 concentrations in drained boreholes, and suppressed O_2 concentrations.

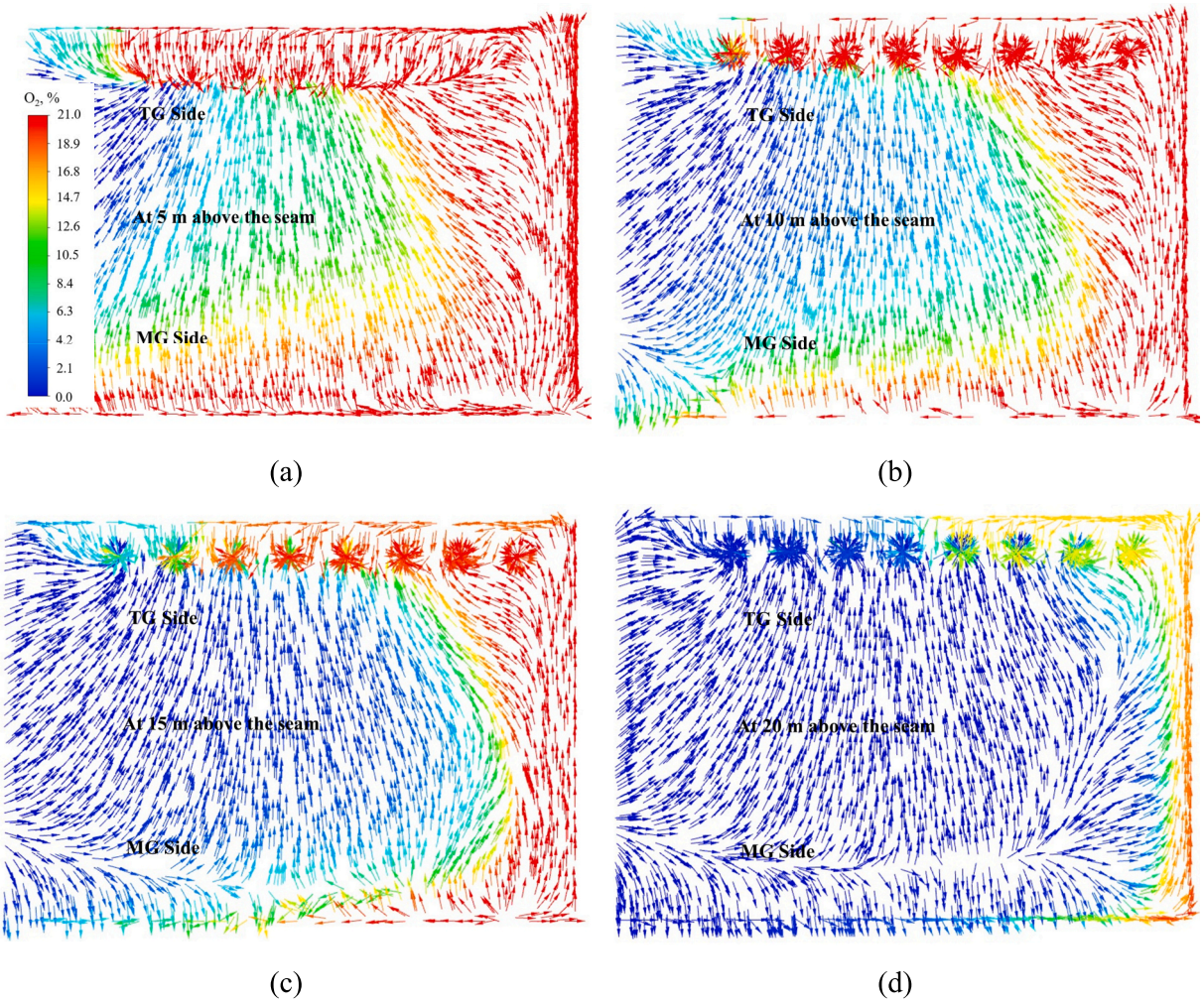

Fig. 17. O_2 migration pathways from the face to tailgate boreholes around the tailgate corner at different goaf heights in plan views: (a) 5 m, (b) 10 m, (c) 15 m, and (d) 20 m above the seam. Flow vectors are coloured by the O_2 concentration.

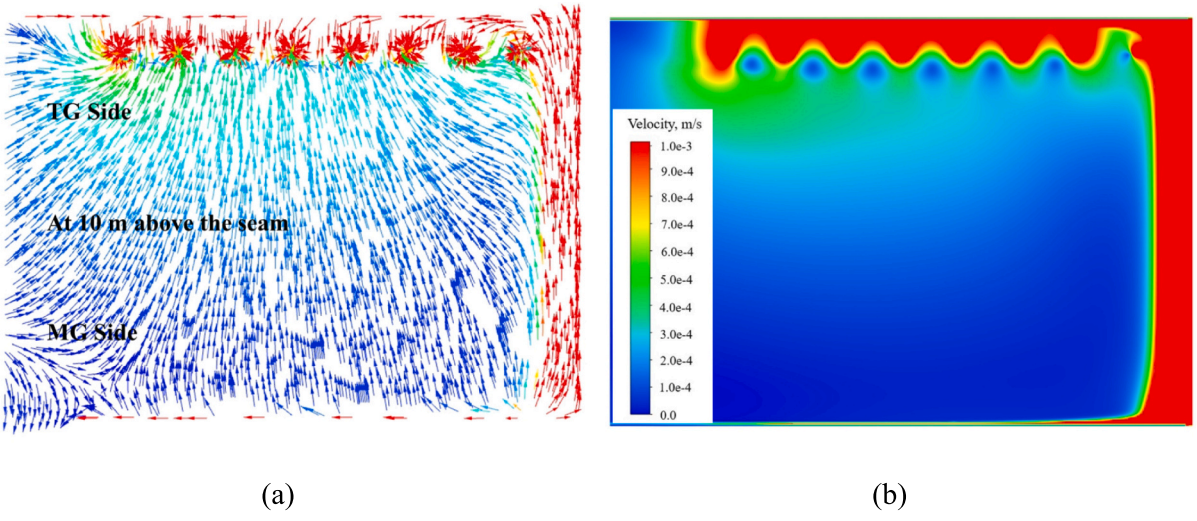

Fig. 18. (a) Goaf gas flow velocity vectors and (b) velocity contours at the borehole completion depth (10 m above the seam).

4.3. Comparison with existing models

While the paper focuses on Australian mines, it would be valuable to compare the simulation results and methodologies with those from mines in other countries, as mining conditions, regulations, and geological characteristics can vary significantly. Previous research mainly aimed to improve drainage efficiency by analysing gas flow rate and goaf drainage locations. However, the composition of captured gas

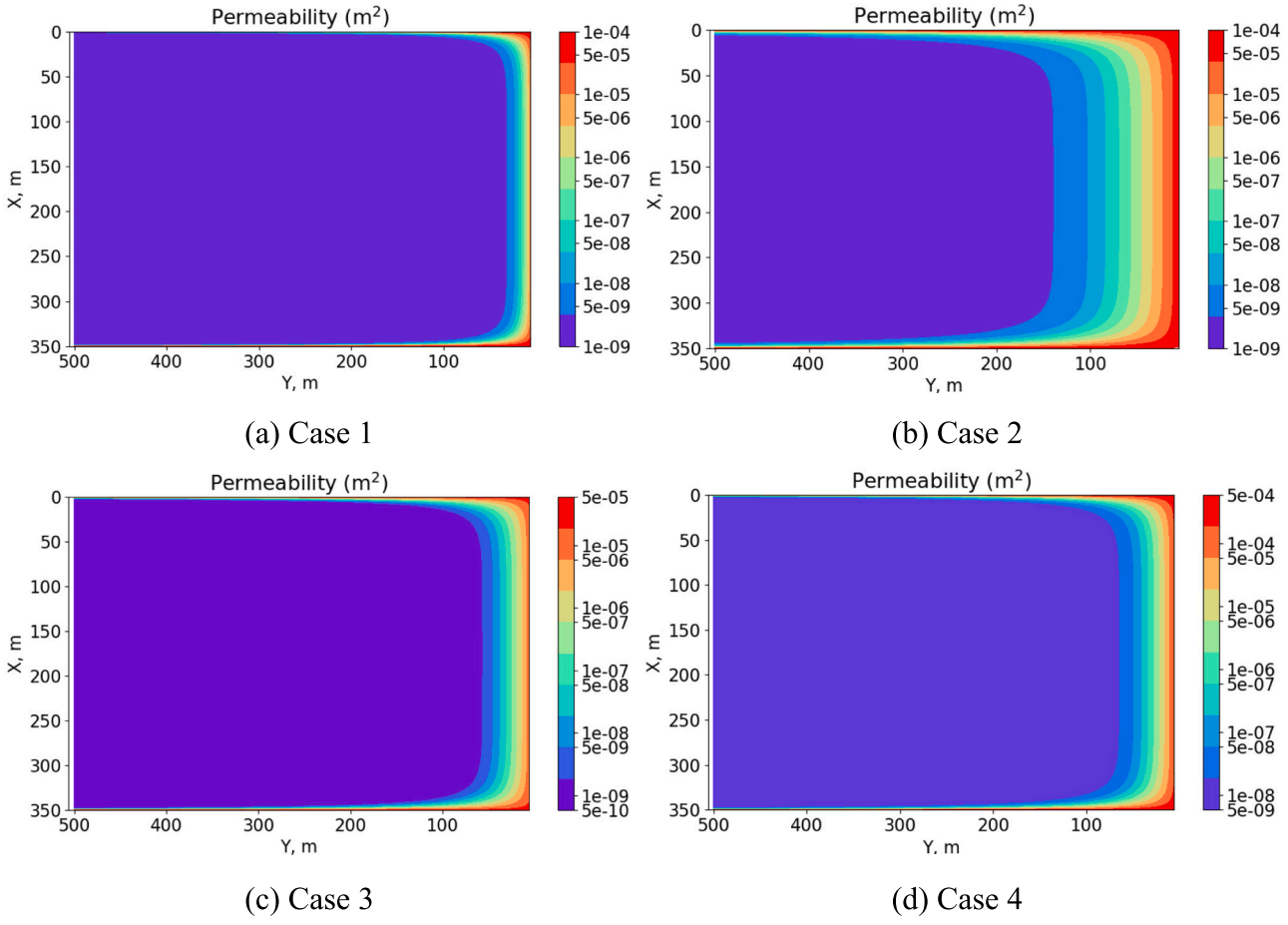

Fig. 19. Different goaf permeability distribution scenarios at 10 m above the seam: (a) Case 1, (b) Case 2, (c) Case 3 and (d) Case 4.

and goaf drainage effects on goaf atmosphere during its production period has not been well understood (Si and Belle, 2019). The primary approach in this study involves using a CFD model to visualize gas mixture distribution and gas flow patterns in the goaf. CFD modelling is a widely used fluid flow simulation technology, but compared with CFD models in similar studies, this paper comprehensively and intuitively analyses the impact of intensive vertical boreholes on the goaf atmosphere. This would involve assessing the accuracy, computational efficiency, and scalability of the proposed CFD model in comparison to existing ones.

This paper not only aims to understand the goaf atmosphere but also investigates the pathways of leaked air from the working face to the goaf. When suction pressure is applied at the top of the tailgate side boreholes, the leaked air from the maingate entry initially travels along the maingate side edge for a certain distance before flowing through the 'high permeability channel' along the working face and tailgate side edge, where it is eventually extracted by operating vertical boreholes. This CFD modelling provides a comprehensive visualization of these airflow pathways and validates the previously proposed conceptual model (Fig. 2) conjectures based solely on back analysis results. In contrast to earlier models that did not consider the impact of goaf gas drainage by CSIRO, as illustrated in Fig. 1, the leaked air travels a greater distance along the maingate side, and some of the leaked ventilation air circulates along the goaf edge towards the tailgate entry, instead of simply exiting directly from the tailgate entry. Therefore, it becomes evident that the influence of intensive vertical boreholes on the goaf atmosphere cannot be disregarded.

Furthermore, this paper delves into the investigation of goaf atmosphere under different natural goaf characteristics. While other studies (e.g., Worrall Jr, 2012; Saki, 2016) also analysed the impact of goaf permeability, coal seam gas emissions and other geological factors on the goaf atmosphere. They have not considered the simultaneous effect of intensive goaf gas drainage. Additionally, the goaf permeability they considered was limited to numerical increases or decreases (e.g., 10%, 20%) and did not consider the impact of different changing trends. Moreover, gas emissions in these studies were assumed to be uniformly emitted into the goaf. In contrast, this paper considers various gas emission rate trends based on in-situ conditions, and the area closer to the face has a higher gas emission rate, which gradually decreases with the increasing distance from the face. This comprehensive analysis of gas flow patterns and its natural characteristics can help engineers optimize the goaf gas drainage design, thereby improving the drainage efficiency and ensuring mine safety.

This study mainly relies on field back analysis results to establish and calibrate the CFD model. The results of collecting and analysing field data are used as input conditions for CFD modelling, such as goal permeability and gas emission setting, and then the simulation results obtained by the model are compared with the field data to ensure the accuracy of the model. The methodologies employed in constructing this model can be adapted to different cases involving diverse mining conditions and geological characteristics. Since existing models are typically based on specific case studies, it is crucial to verify the accuracy and practical applicability of each model or method. In comparison with existing models, the CFD model presented in this paper incorporates a more extensive analysis of field data to provide an analytical approach for industrial-scale problems. However, this paper uses a simplified geometry model to ensure the modelling computational efficiency, which lacks the ability to explain complex geological conditions. When compared with other studies (e.g., Karacan et al., 2007a; Karacan, 2009c; Guo et al., 2012) investigating gas migration in underground

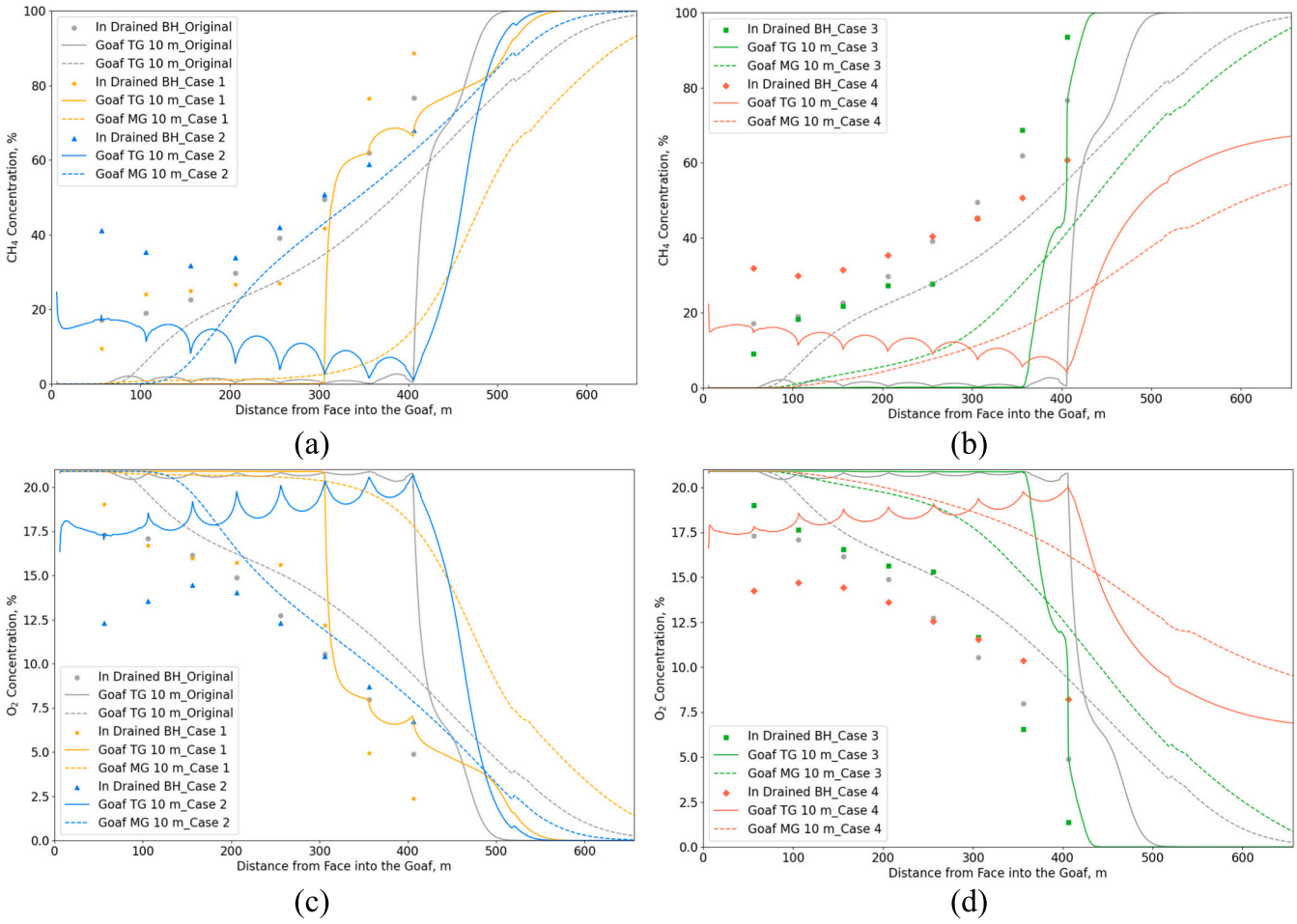

Fig. 20. Impact of goaf permeability on the goaf atmosphere and gas composition in drained boreholes: (a) CH4 concentrations for Cases Original, 1, and 2, (b) CH4 concentrations for Cases Original, 3, and 4, (c) O2 concentrations for Cases Original, 1, and 2, and (d) O2 concentrations for Cases Original, 3, and 4.

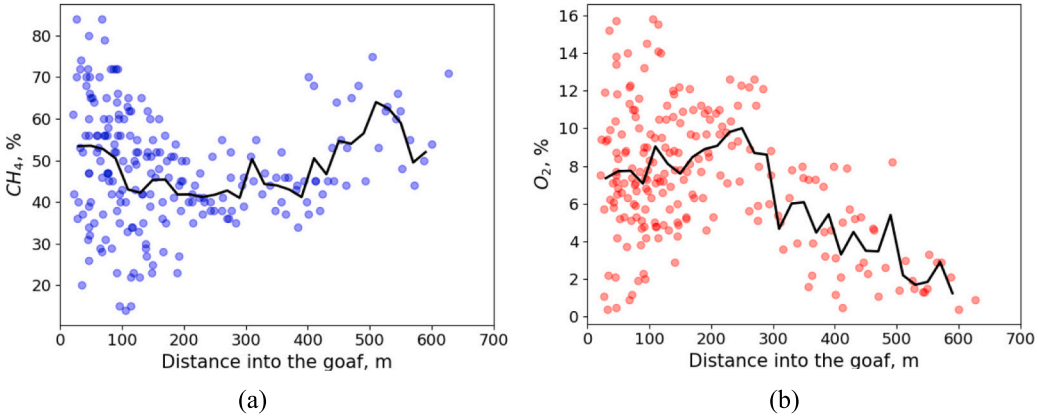

Fig. 21. Goaf gas profiles (a) CH_4 and (a) O_2 along the tailgate side goaf at a longwall panel adjacent to LWA (Si and Belle, 2019).

mines, this paper does not delve into a detailed examination of factors affecting gas migration pathways, such as strata properties and geological structure. Therefore, further research can consider more complex geological structures by combining geological modelling and reservoir modelling.

5. Conclusions

This paper presents a method that applies CFD simulation to analyse the infiltration of leakage air from the working face into the deep goaf under intensive vertical borehole drainage on the tailgate side goaf. The CFD model is based on a generic geometry from an Australian underground coal mine and calibrated based on goaf gas drainage data collected at the field, e.g., suction pressure, flow rate, and gas composition. Additionally, the simulation results of this model can potentially reflect the true physics of ventilation airflow, goaf gas emissions, and gas drainage impact on the goaf atmosphere. Due to the suction pressure applied on the top of vertical boreholes, the O_2 level on the tailgate side

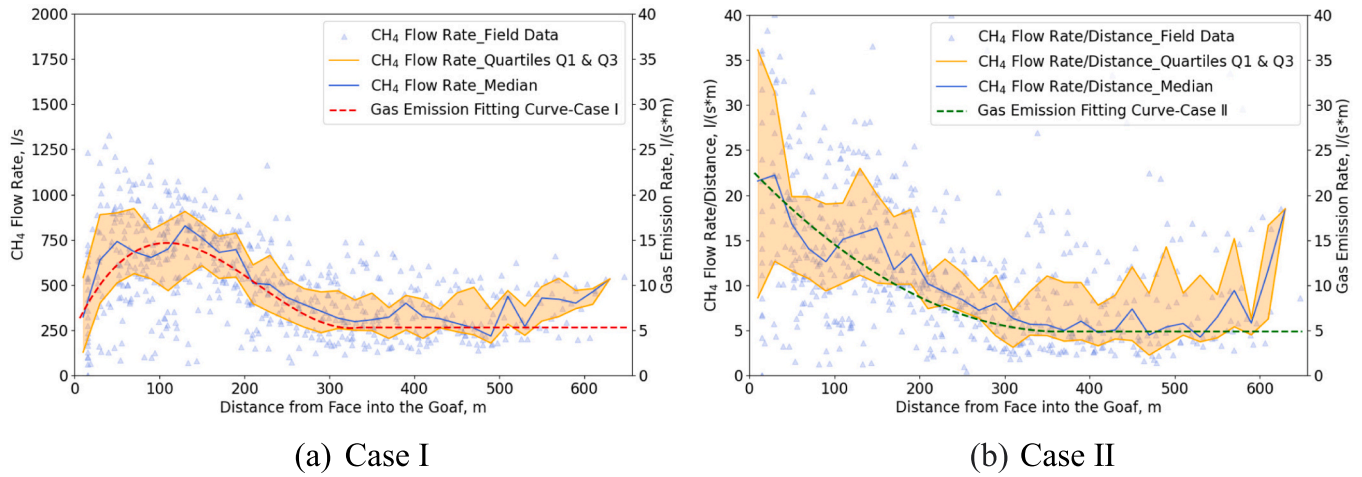

Fig. 22. Different gas emission scenarios at the top layer: (a) Case I and (b) Case II.

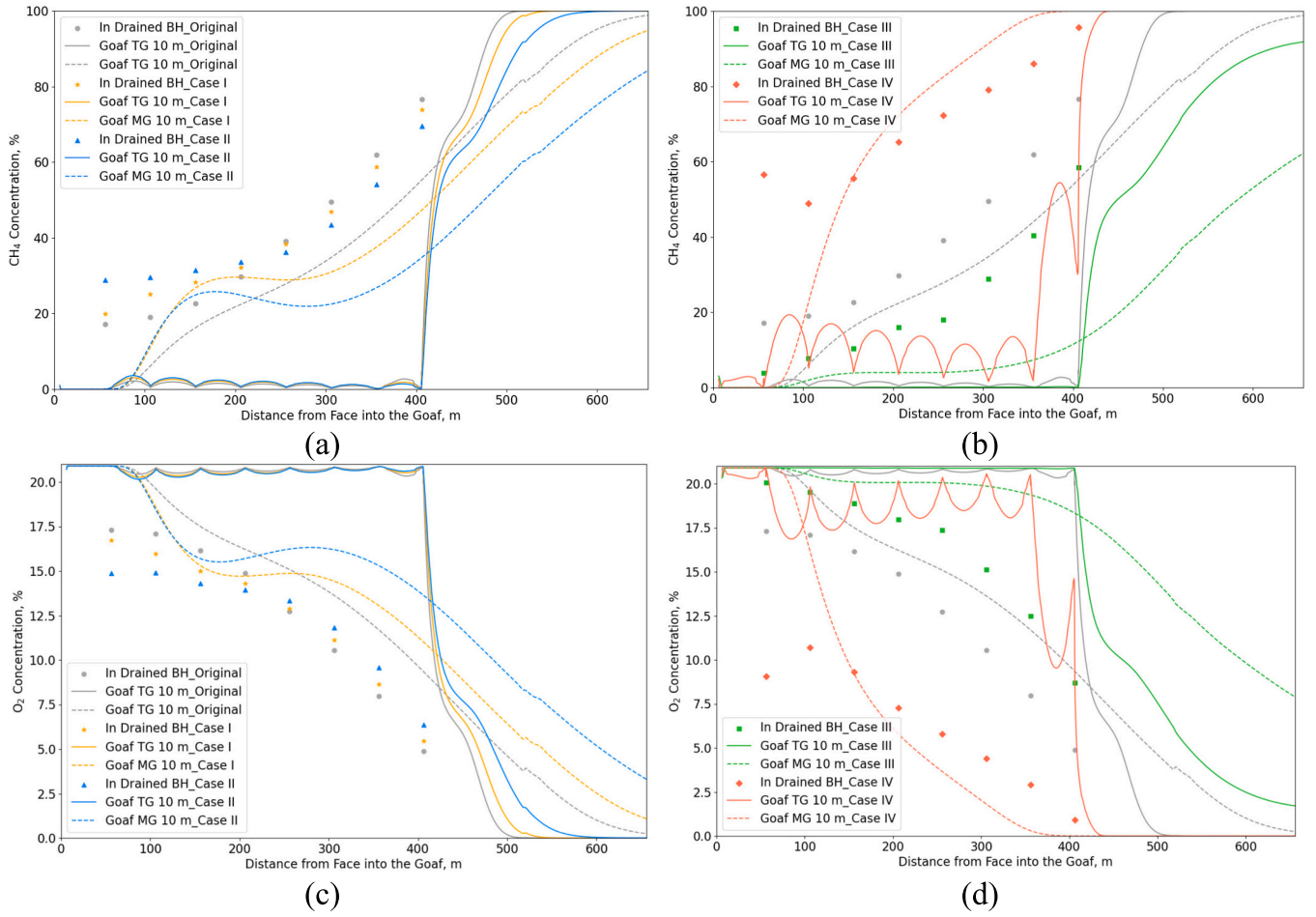

Fig. 23. Impact of gas emission rate on the goaf atmosphere and gas composition in drained boreholes: (a) CH_4 concentrations for Cases Original, I, and II, (b) CH_4 concentrations for Cases Original, III, and IV, (c) O_2 concentrations for Cases Original, I, and II, and (d) O_2 concentrations for Cases Original, III, and IV.

goaf is reported to be much higher than the maingate side, which is consistent with field observations due to the goaf drainage strategy applied. Moreover, the O_2 concentration found in drained boreholes show a decreasing trend with distance from the working face. The O_2 concentration is less than that found in the goaf near the seam, which is explained by the high-purity gas inflow to the boreholes from the overlying strata.

Furthermore, the detailed analysis of the gas flow patterns in the goaf illustrates that the majority of leaked air from the face travels along the goaf edge near the tailgate. The uncaved or unconsolidated goaf at the tailgate side edge provides a fast flow channel for the leaked air to migrate to the boreholes at different goaf locations. This suggests that the goaf is relatively well-compacted at the central part, and the ventilation air does not directly penetrate the central compacted part.

Instead, it takes a 'detour' from the goaf edge with high permeability channels and then circulates back to the boreholes, driven by the suction pressure of these boreholes. The air leakage flow pathways in the goaf from the calibrated CFD model is also consistent with the goaf conceptual model in Fig. 2 based on the back analysis results of field data (Xiang et al., 2021).

However, the findings presented in Section 3 of this paper are based on the goaf gas distribution likelihood under specific permeability and gas emission settings. This is due to the unavailability of relevant data about goaf characteristics, and only gas drainage data from goaf boreholes could be used for calibration. As a result, the impact of different permeability distributions and gas emission inputs on the goaf atmosphere are discussed in Section 4. The decline rate and magnitude of goaf permeability may have a significant impact on goaf gas profiles. Besides, the O_2 concentration found in boreholes close to the face (e.g., BH1 to BH3) may show large variations with different goaf compaction levels, which was also observed in field goaf drainage data (Fig. 16 and Fig. 21). Moreover, the sensitivity of goaf atmosphere response to gas emission rate was analysed. Within a certain range, as the gas emission rate change more sharply in the direction of the working face, higher CH_4 content is observed in the goaf. Thus, boreholes located near the working face can extract more CH_4 and less O_2 in these cases.

In conclusion, the goaf gas drainage impact on the goaf atmosphere needs to be further refinement through numerical simulation research, and a balance point between goaf drainage efficiency and associated operational risks needs to be found in goaf management. It is concerned that excessive goaf drainage pressure or inadequately managed boreholes may reduce gas purity and incur gas explosion/sponcom hazards (Belle, 2017; Si and Belle, 2019). Reduced methane purity in goaf drainage indicates more ventilation air migrating from the face to deeper goaf, which increases gas explosion/sponcom risks, as the presence of oxygen is a prerequisite for these catastrophic mining hazards. Additionally, air contamination complicates the utilisation of captured gas, sometimes requiring additional costs to further purify the methane, forcing operators to directly burn the gas despite the high cost of drainage boreholes. Furthermore, these risks may change dynamically according to various goaf drainage performance and goaf natural characteristics. Consequently, the simulation results of this CFD modelling can be employed to access the potential risks associated with intensive vertical boreholes in further research and assist engineers in implementing appropriate methods to mitigate these risks, such as inertisation strategies.

Author statements

Yuehan Wang: Data curation, Analysis, Writing- Original draft preparation.

Guangyao Si: Conceptualization, Methodology, Supervision.

Joung Oh: Conceptualization, Methodology, Supervision, Funding acquisition.

Bharath Belle: Conceptualization, Writing- Reviewing and Editing, Resources.

On behalf of all co-authors, I declare above information is true and accurate.

Declaration of Competing Interest

None.

Data availability

Data will be made available on request.

Acknowledgements

The authors would like to thank Australian Coal Association Research Program (ACARP) C29017 and C34011 for supporting this work. The authors would also like to thank Australian Research Council Linkage Program (LP200301404) for sponsoring this research.

References

Balusu, R., Humphries, P., Harrington, P., Wendt, M., Xue, S., 2002. Optimum inertisation strategies. In: Proceedings of Queensland Mining Industry Health and Safety Conference, Townsville, Australia, pp. 133–144.

Balusu, R., Neil, R., Ron, P., Tim, H., Shen, Z., Haruko, I., 2004. Optimisation of longwall goaf gas drainage & control system. ACARP Rep. C10017.

Balusu, R., Tuffs, N., Peace, R., Xue, S., 2005. Longwall goaf gas drainage and control strategies for highly gassy mines. In: 8th International Mine Ventilation Congress, pp. 201–209.

ANSYS Inc, 2020. ANSYS Fluent Theory Guide (in Italics). ANSYS Inc, Canonsburg, Pennsylvania.

Balusu, R., Belle, B., Tanguturi, K., 2019. Development of goaf gas drainage and inertisation strategies in 1.0-km and 3.0-km long panels. Mining, Metall. Expl. 36 (6), 1127–1136.

Belle, B., 2014. Evaluation of Barometric Pressure (BP) and Cage Effect on Longwall Tailgate Gas Levels. In: Proceedings of the 10th International Mine Ventilation Congress, Sun City, pp. 501–511.

Belle, B., 2017. Optimal goaf hole spacing in high production gassy Australian longwall mines- operational experiences. In: Proceedings of Australian Mine Ventilation Conference, Brisbane, Australia, pp. 28–30. August.

Brodny, J., Tutak, M., 2021. Applying computational fluid dynamics in research on ventilation safety during underground hard coal mining: a systematic literature review. Process. Saf. Environ. Prot. 151, 373–400.

Brodny, J., Tutak, M., Anderson, J., 2018. Analysis of influence of types of rocks forming the goaf with caving on the physical parameters of air stream flowing through these gob and adjacent headings. Mechanika 24 (1), 43–49.

Esterhuizen, G.S., Karacan, C.Ö., 2005. Development of numerical models to investigate permeability changes and gas emission around longwall mining panel. In: Alaska Rocks 2005, The 40th US Symposium on Rock, OnePetro.

Esterhuizen, G.S., Karacan, C.Ö., 2007. Methodology for determining gob permeability distributions and its application to reservoir modeling of coal mine longwalls. In: 2007 SME Annual Meeting and Exhibit, February 25–28. Denver, CO, pp. 07–78.

Gao, J., Wang, H., 2010. Influence of permeability distribution on airflow field of leakage in gob. China Safety Sci J 30 (3), 81–85.

Gao, J., Li, X., Cui, Y., 2013. Numerical simulation for airflow and gas distribution regulation in the goaf of mechanized working face. J. Saf. Environ. 13 (2), 164–168.

Guo, H., Adhikary, D.P., Craig, M.S., 2008. Simulation of mine water inflow and gas emission during longwall mining. Rock Mech. Rock. Eng. 42 (1), 25–51.

Guo, H., Yuan, L., Shen, B., Qu, Q., Xue, J., 2012. Mining-induced strata stress changes, fractures and gas flow dynamics in multi-seam longwall mining. Int. J. Rock Mech. Min. Sci. 54, 129–139.

Guo, H., Todhunter, C., Qu, Q., Qin, Z., 2015. Longwall horizontal gas drainage through goaf pressure control. Int. J. Coal Geol. 150-151, 276–286.

Karacan, C.Ö., 2009. Prediction of Porosity and Permeability of Caved Zone in Longwall Gobs. Transp. Porous Media 82 (2), 413–439.

Karacan, C.Ö., 2009b. Degasification System selection for US Longwall Mines using an Expert Classification System. Comput. Geosci. 35 (3), 515–526.

Karacan, C.Ö., 2009c. Reconciling Longwall Gob Gas Reservoirs and Venthole Production Performances using Multiple Rate Drawdown well Test Analysis. Int. J. Coal Geol. 80 (3–4), 181–195.

Karacan, C.Ö., 2010. Prediction of porosity and permeability of caved zone in longwall gobs. Transp. Porous Media 82 (2), 413–439.

Karacan, C.Ö., Diamond, W.P., Schatzel, S.J., Garcia, F., 2006. Development and Application of Reservoir Models for the Evaluation and Optimization of Longwall Methane Control Systems. National Institute for Occupational Safety and Health, Pittsburgh Research Laboratory.

Karacan, C.Ö., Esterhuizen, G.S., Schatzel, S.J., Diamond, W.P., 2007a. Reservoir Simulation-based Modelling for characterizing longwall methane emissions and gob gas venthole production. Int. J. Coal Geol. 71 (2–3), 225–245.

Karacan, C.Ö., Esterhuizen, G.S., Schatzel, S.J., Diamond, W.P., 2007b. Numerical Analysis of the Impact of Longwall Panel Width on methane Emissions and Performance of Gob Gas Ventholes. Int. J. Coal Geol. 71 (2–3), 225–245.

Karacan, C.Ö., Ruiz, F.A., Cotè, M., Phipps, S., 2011. Coal mine methane: a review of capture and utilization practices with benefits to mining safety and to greenhouse gas reduction. Int. J. Coal Geol. 86 (2–3), 121–156.

Karacan, C.Ö., Goodman, G.V., Phipps, S., 2012. Development of an integrated reservoir and geomechanical model for optimal design of methane drainage and gob ventilation systems. Int. J. Coal Geol. 94, 190–211.

Liu, H., Wu, C., Shi, Y., 2011. Locating method of fire source for spontaneous combustion of sulfide ores. J. Cent. S. Univ. Technol. 18 (4), 1034–1040.

Liu, J., Wu, N., Si, G., Zhao, M., 2021. Experimental study on mechanical properties and failure behaviour of the pre-cracked coal-rock combination. Bull. Eng. Geol. Environ. 80, 2307–2321.

Lunarzewski, L.W., 1998. Gas emission prediction and recovery in underground coal mines. Int. J. Coal Geol. 35 (1–4), 117–145.

Marts, J.A., Gilmore, R.C., Brune, J.F., Bogin Jr., G.E., Grubb, J.W., Saki, S., 2014. Dynamic gob response and reservoir properties for active longwall coal mines. Min. Eng. 66 (12), 59–66.

Qin, Z., Yuan, L., Guo, H., Qu, Q., 2015. Investigation of longwall goaf gas flows and borehole drainage performance by CFD simulation. Int. J. Coal Geol. 150, 51–63.
Qin, J., Qu, Q., Guo, H., 2017. CFD simulations for longwall gas drainage design optimisation. Int. J. Min. Sci. Technol. 27 (5), 777–782.
Qu, Q., Balusu, R., Belle, B., 2022. Specific Gas Emissions in Bowen Basin Longwall mines, Australia. Int. J. Coal Geol. 261, 104076.
Ren, T., Balusu, R., Claassen, C., 2011. Computational fluid dynamics modelling of gas flow dynamics in large longwall goaf areas. In: Proceedings of 35th APCM Symposium - Application of Computers and Operations Research in the Minerals Industry, pp. 603–613.
Saki, S.A., 2016. Gob Ventilation Borehole Design and Performance Optimization for Longwall Coal Mining Using Computational Fluid Dynamics (Doctoral dissertation).. Colorado School of Mines.
Si, G., Belle, B., 2019. Performance analysis of vertical goaf gas drainage holes using gas indicators in Australian coal mines. Int. J. Coal Geol. 216, 103301.
Si, G., Durucan, S., Jamnikar, S., Lazar, J., Abraham, K., Korre, A., Shi, J.Q., Zavšek, S., Mutke, G., Lurka, A., 2015a. Seismic monitoring and analysis of excessive gas emissions in heterogeneous coal seams. Int. J. Coal Geol. 149, 41–54.
Si, G., Jamnikar, S., Lazar, J., Shi, J.Q., Durucan, S., Korre, A., Zavšek, S., 2015b. Monitoring and modelling of gas dynamics in multi-level longwall top coal caving of ultra-thick coal seams, part I: Borehole measurements and a conceptual model for gas emission zones. Int. J. Coal Geol. 144, 98–110.
Si, G., Wang, Y., Xiang, Z., Chalmers, D., 2021. Appraisal of gas indicators from goaf drainage holes for spontaneous combustion and explosion risk management. ACARP report C29017.
Szurgacz, D., Brodny, J., 2020. Adapting the powered roof support to diverse mining and geological conditions. Energies 13 (2), 405.
Tanguturi, K., Balusu, R., Morla, R., Khanal, M., 2012. Effect of buoyancy on methane gas distribution and gas control strategies at tailgate region in a gassy coal mine. In: In: 9th International Conference on CFD in the Minerals and Process Industries. CSIRO, Melbourne, Australia.
Tomita, S., Deguchi, G., Matsuyama, S., Li, H., Kawahara, H., 2003. Development of a simulation program to predict gas emission based on 3D stress analysis. In: In Proceedings of 30th International Conference of Safety in Mines Research Institutes, South African Institute of Mining and Metallurgy, pp. 69–76.
Tutak, M., Brodny, J., 2017. Analysis of influence of goaf sealing from tailgate on the methane concentration at the outlet from the longwall. In: IOP Conference Series: Earth and Environmental Science, 95, p. 042025.
Tutak, M., Brodny, J., Szurgacz, D., Sobik, L., Zhironkin, S., 2020. The impact of the ventilation system on the methane release hazard and spontaneous combustion of coal in the area of exploitation - a case study. Energies 13 (18), 4891.
Wachel, E.W., 2012. Establishing Longwall Gob Porosity from Compaction in Western Coal Mines. Masters Report, Colorado School of Mines.
Wang, Y., Si, G., Xiang, Z., Oh, J., Belle, B., Webb, D., 2022a. A theoretical goaf resistance model based on gas production analysis in goaf gas drainage. Int. J. Coal Geol. 264, 104140.
Wang, Y., Si, G., Belle, B., Oh, J., Xiang, Z., 2022b. A theoretical goaf resistance model based on goaf gas drainage data. In: AusIMM mine ventilation conference 2022, Gold Coast, Australia, pp. 436–446. October 10-12, 2022.
Worrall Jr., D.M., 2012. Modeling Gas Flows in Longwall Coal Mines Using Computational Fluid Dynamics (Doctoral dissertation).. Colorado School of Mines.
Xiang, Z., Si, G., Wang, Y., Belle, B., Webb, D., 2021. Goaf gas drainage and its impact on coal oxidation behaviour: a conceptual model. Int. J. Coal Geol. 248, 103878.
Yang, X., Zhou, F., Chen, Y., Xie, D., Liu, C., 2014. Numerical simulation of heat accumulation and gas explosion risk of ventilation air in goaf. J. China Coal Soc. 39 (9), 1846–1852.
Yuan, L., Smith, A.C., Brune, J.F., 2006. Computational fluid dynamics study on the ventilation flow paths in longwall gobs. In: Proceedings of the 11th U.S./North American Mine Ventilation Symposium, University Park, Pennsylvania, pp. 591–598. June 5-7, 2006.
Zhang, C., Tu, S., Zhang, L., Bai, Q., Yuan, Y., Wang, F., 2016. A methodology for determining the evolution law of gob permeability and its distributions in longwall coal mines. J. Geophys. Eng. 13 (2), 181–193.
Zhang, C., Tu, S., Zhao, Y., 2019a. Compaction characteristics of the caving zone in a longwall goaf: a review. Environ. Earth Sci. 78, no. 1.
Zhang, J., Zhang, H., Ren, T., Wei, J., Liang, Y., 2019b. Proactive inertisation in longwall goaf for coal spontaneous combustion control-A CFD approach. Saf. Sci. 113, 445–460.